J. Fluid Mech. (2005), *vol.* 544, *pp.* 243–275.
doi:10.1017/S0022112005006622 Printed in the United Kingdom

Steady deformation and tip-streaming of a slender bubble with surfactant in an extensional flow

By M. R. BOOTY AND M. SIEGEL

Department of Mathematical Sciences, New Jersey Institute of Technology, Newark, NJ 07102, USA

(Received 20 November 2004 and in revised form 25 May 2005)

Slender-body theory is used to investigate the steady-state deformation and time-dependent evolution of an inviscid axisymmetric bubble in zero-Reynolds-number extensional flow, when insoluble surfactant is present on the bubble surface. The asymptotic solutions reveal steady ellipsoidal bubbles covered with surfactant, and, at increasing deformation, solutions distinguished by a cylindrical surfactant-free central part, with stagnant surfactant caps at the bubble endpoints. The bubble shapes are rounded near the endpoints, in contrast to the pointed shapes found for clean inviscid bubbles. Simple expressions are derived relating the capillary number Q to the steady bubble slenderness ratio ϵ. These show that there is a critical value Q_c above which steady solutions no longer exist. Equations governing the time-evolution of a slender inviscid bubble with surfactant, valid for large capillary number, are also derived. Numerical solutions of the slender bubble equations for $Q > Q_c$ exhibit spindle shapes with tip-streaming filaments.

1. Introduction

The deformation and breakup of a drop or bubble in an imposed extensional flow at low Reynolds number is a fundamental process in fluid mechanics, with applications to the formation, stability and rheology of emulsions. The systematic study of drop deformation and breakup was initiated by Taylor (1934), who used a four-roller mill to subject single drops suspended in a highly viscous fluid to shearing and straining flows. Taylor's experiments revealed the existence of steady rounded and pointed drops, as well as bursting drops of each type, depending on the ratio $\lambda = \mu_i/\mu$ of drop to suspending liquid viscosity and the capillary number $Q = \mu G a/\sigma$, where G is the imposed strain rate, σ is the surface tension, and a is a length scale equal to the radius of a spherical drop with the same volume. Subsequent experiments by Rumscheidt & Mason (1961), Torza, Cox & Mason (1972), Grace (1982) and Bentley & Leal (1986) have confirmed and extended Taylor's results. In many of these early studies, the word 'bursting' refers to the non-existence of a steady drop shape when the applied shear or strain exceeds a critical value, rather than the actual breakup of the drop. Reviews by Acrivos (1983) and Rallison (1984) summarize some of the early experiments, while Stone (1994) describes more recent developments.

Much work has focused on drop deformation for clean fluid systems in which interfacial tension gradients are absent. For these 'clean' drops, experiments, asymptotic analysis, and numerical simulations have revealed a relatively complete picture of the deformation and breakup, for which there is good agreement between

theory and experiment. Many of the theoretical developments have exploited the slenderness of the deformed drop profile. For example, Buckmaster (1972) presented a mathematically detailed treatment of an inviscid bubble in zero-Reynolds-number axisymmetric straining flow by employing slender-body theory to compute the leading-order solution in the slenderness ratio $\epsilon = b/l$, where b is the height and l the half-length of the bubble. Buckmaster's analysis showed that steady pointed bubble solutions exist for arbitrarily large capillary number. Numerical calculations of Youngren & Acrivos (1976) confirm this conclusion, at least over a finite range of capillary number. Acrivos & Lo (1978) refined Buckmaster's analysis and further showed that the inviscid bubble solutions are stable. These results suggest that, in the absence of inertia, an initially spherical inviscid drop in an extensional flow attains a steady shape, regardless of the magnitude of the applied strain.

Buckmaster (1973) and Acrivos & Lo (1978) further extended the treatment based on slender-body theory to the case when the viscosity ratio λ is not identically zero, but is chosen according to the scaling $\lambda = O(\epsilon^2)$. They find that the bubble still deforms into a steady slender shape provided that the strain rate (or equivalently the capillary number) is below a critical value given by $Q_c = G_c \mu a/\sigma \approx 0.148\lambda^{-1/6}$ (this criterion was also found by Taylor 1964). For strain rates in excess of this value, steady drop solutions no longer exist, and a time-dependent drop bursts. This result is in close agreement with the experiments of Grace (1982), who found that relatively large strain rates were required for drop breakup when $\lambda \ll 1$, with the critical value $Q_c = G_c \mu a/\sigma$ being proportional to $\lambda^{-0.16}$. A similar scenario is found for the bursting of a slender inviscid drop in a non-zero-Reynolds-number flow. Thus, the phenomenon of breakup is associated with the non-existence of a steady solution when the relevant non-dimensional group (i.e. $Q = G\mu a/\sigma$) lies beyond a critical value, rather than the instability of an existing steady state when the control parameter exceeds a critical value. Extensions of slender-body theory to time-dependent drop evolution can be found in Hinch (1980) and Sherwood (1984). A study of time-dependent drop evolution in the near-sphere limit is given by Barthes-Biesel Acrivos (1973).

The present paper is concerned with the application of slender-body theory to inviscid bubbles (i.e. $\lambda = 0$) in extensional flow, in the case when insoluble surfactant is present on the drop interface. Variations in interfacial surface tension that are introduced by surfactant often have dramatic effects in free-surface flows. An example is the phenomenon of tip-streaming, first observed by Taylor (1934), but only recently associated with the presence of surfactant. Tip-streaming is a mode of breakup in an extensional flow where a deformed drop (often featuring cusplike ends) emits thin threads or small daughter droplets into the exterior fluid (de Bruijn 1993; Janssen, Boon & Agterof 1994, 1997). The strain rate required for this type of breakup is typically much less than that required for the usual mode of breakup for a clean surface, or fracture, in which a drop ruptures into two or three pieces of similar size, with a few tiny satellite drops in between (de Bruijn 1993). The droplets produced in tip-streaming are much smaller than their parent drops, typically with radii two orders of magnitude less, and exhibit a greatly reduced surface tension. The experiments of de Bruijn (1993) and Janssen *et al.* (1994, 1997) provide strong evidence that interfacial tension gradients due to the presence of surfactant play a critical role in tip-streaming. As further evidence of this, numerical simulations (Eggleton, Tsai & Stebe 2001) using a boundary-integral method show transient drop shapes with pointed tips, from which thin threads are emitted, evoking the tip-streaming observed in experiments. Other numerical studies on the influence of surfactant in drop deformation and breakup include Stone & Leal (1990) and Milliken, Stone & Leal (1993).

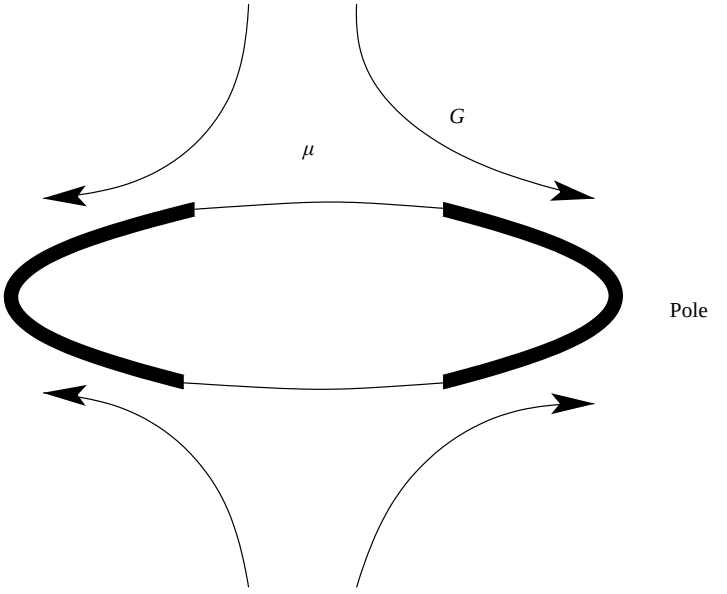

FIGURE 1. Illustration of a stagnant-cap bubble. The stagnant surfactant-caps are denoted by dark curves.

Unlike the surfactant-free or 'clean' flow problem, there has been no theoretical analysis on slender inviscid drops with surfactant in an extensional flow. The aim of this paper is to fill the gap in theory by providing a detailed mathematical analysis, based on slender-body theory, as an adjunct to experiments and numerical simulations for finite capillary number Q. The analysis reveals some interesting mathematical and physical features. For bubbles with sufficiently large deformation, the steady solutions are distinguished by a cylindrical surfactant-free central part, with localized 'surfactant caps' in the neighbourhood of the bubble endpoints (see figure 1). When surface diffusion of surfactant is negligible compared to surface transport, a steady surface with surfactant is stagnant, i.e. a no-slip condition is satisfied there. Stagnant-cap bubbles have been investigated for a steadily translating spherical drop in an otherwise quiescent fluid (Sadhal & Johnson 1983) and in exact solutions for two-dimensional strained bubbles (Siegel 1999). The boundary-value problem associated with a stagnant-cap bubble in Stokes flow is characterized by mixed boundary conditions at the bubble surface, and free boundary curves that define the edges of the cap. The location of these curves must be determined as part of the solution. Common features in the asymptotic analysis of such codimension-two free-boundary problems are discussed in Howison, Morgan & Ockendon (1997).

Our asymptotic analysis yields simple expressions for steady bubble solution branches for both surfactant-covered bubbles (equation (3.37)) and stagnant-cap bubbles (equation (3.70)), in the inviscid limit. It also reveals the existence and magnitude of a critical capillary number Q_c, above which steady slender solutions no longer exist. In this respect, the effect of surfactant is analogous to that of finite interior drop viscosity or exterior fluid inertia. However, our results suggest that for sufficiently small values of the viscosity ratio λ, surfactant dominates over interior drop visicosity as a mechanism for bursting.

Equations governing the time-evolution of a slender inviscid bubble in an axisymmetric straining flow are also presented, in the case for which insoluble

surfactant acts on the bubble surface. The equations are valid for large capillary number, in a sense which is quantified in § 5. Numerical simulations of these equations show unsteady solutions that exhibit transient pointed shapes with tip-streaming threads, like those observed in experiments (see e.g. de Bruijn 1993; Eggers 1997).

The rest of the paper is organized as follows. The governing equations are presented in § 2. Slender-body theory for steady-state inviscid bubbles with surfactant is developed in § 3. The case of a bubble that is completely covered in surfactant is first considered in § 3.1, where an asymptotic solution is developed in integer powers of $\ln(1/\epsilon)$, as occurs for a solid slender body in an extensional Stokes flow (Tillet 1970). However, unlike flow around a solid of arbitrary shape, a simple solution is found that is valid to all integer powers in $\ln(1/\epsilon)$. The case of partially covered, or stagnant-cap, bubbles is treated in § 3.2, and the steady response curves are characterized in § 3.3. The slender-bubble solutions found in § 3 have a non-uniformity at the bubble endpoints, and this is remedied in § 4, where a local analysis verifies that the endpoints are rounded. The time-dependent evolution equations and unsteady solutions are presented in § 5, and concluding remarks are presented in § 6. An Appendix presents some details of the slender-body analysis.

2. Governing equations

The governing equations for Stokes flow of a fluid with constant viscosity μ are

$$\nabla \cdot \boldsymbol{u} = 0, \quad \nabla p = \mu \nabla^2 \boldsymbol{u}, \tag{2.1}$$

where $\boldsymbol{u}$ is the fluid velocity and p is the pressure. The boundary condition at infinity is that the flow approaches a state of uniaxial extension with imposed strain rate G and a constant pressure which is taken to be zero,

$$\boldsymbol{u} \to G\big(-\tfrac{1}{2} r \boldsymbol{e}_r + z \boldsymbol{e}_z\big), \quad p \to 0 \text{ as } |\boldsymbol{x}| \to \infty. \tag{2.2}$$

We look for axisymmetric solutions in a cylindrical polar coordinate system r, θ, z, in which the bubble surface is

$$S : r = R(z) \text{ with } R(0) = b, \ \ R(l) = 0. \tag{2.3}$$

The outward normal $\boldsymbol{n}$ oriented from the bubble surface to the surrounding fluid and a unit tangent vector $\boldsymbol{t}$ in a plane of axisymmetry $\theta =$ constant are

$$\boldsymbol{n} = \frac{(1, 0, -R')}{(1 + R'^2)^{1/2}}, \quad \boldsymbol{t} = \frac{(R', 0, 1)}{(1 + R'^2)^{1/2}}. \tag{2.4}$$

When a surfactant adsorbs onto the bubble surface to create a surface concentration Γ, the surface tension reduces from its surfactant-free or clean value σ_0. The simplest model for the dependence of interfacial surface tension σ on surfactant concentration Γ is given by the linear relation (see e.g. Stone & Leal 1990)

$$\sigma = \sigma_0 - (RT)\Gamma, \tag{2.5}$$

where σ_0 is the surface tension in the absence of surfactant, R and T are the surfactant's gas constant (i.e. universal gas constant divided by molecular weight) and the uniform temperature. More precise models incorporate a nonlinear dependence of σ on Γ with the fact that there is an upper bound to the surfactant concentration, denoted by Γ_∞. An equation of state which accounts for these effects is

$$\sigma = \sigma_0 + (RT\Gamma_\infty) \ln\left(1 - \frac{\Gamma}{\Gamma_\infty}\right). \tag{2.6}$$

Since it leads to simpler formulae, the theory developed in this paper will be presented with the linear equation of state, although it is a simple matter to substitute a nonlinear model. An illustrative result using the nonlinear equation is presented in § 3.2.

Axisymmetry implies that σ and Γ are functions of z alone. In the steady state, a balance of stress $\boldsymbol{\tau}$ at the interface requires that

$$[\boldsymbol{\tau}]^{+}_{-} = \sigma(\kappa_\theta + \kappa_z)\boldsymbol{n} - \nabla_s\sigma, \tag{2.7}$$

where $[\cdot]^{+}_{-}$ denotes change across S, κ_θ and κ_z are the principal normal curvatures of S, and ∇_s is the surface gradient operator $\nabla_s = \nabla - \boldsymbol{n}(\boldsymbol{n}\cdot\nabla)$. Since the stress vector for a Newtonian fluid is $\boldsymbol{\tau} = -p\boldsymbol{n} + 2\mu\boldsymbol{e}\cdot\boldsymbol{n}$, where $\boldsymbol{e}$ is the rate of strain tensor, and the fluid in the bubble interior is completely inviscid, the tangential and normal components of (2.7) are

$$\frac{2\mu}{(1+R'^2)}\left(R'\frac{\partial u_r}{\partial r} + (1-R'^2)\tfrac{1}{2}\left(\frac{\partial u_r}{\partial z} + \frac{\partial u_z}{\partial r}\right) - R'\frac{\partial u_z}{\partial z}\right) = \frac{-\sigma'}{(1+R'^2)^{1/2}}, \tag{2.8}$$

$$p_i - p_e + \frac{2\mu}{(1+R'^2)}\left(\frac{\partial u_r}{\partial r} - R'\left(\frac{\partial u_r}{\partial z} + \frac{\partial u_z}{\partial r}\right) + R'^2\frac{\partial u_z}{\partial z}\right) = \frac{\sigma}{R(1+R'^2)^{1/2}}\left(1 - \frac{RR''}{(1+R'^2)}\right), \tag{2.9}$$

where p_i and p_e are the pressure interior and exterior to the bubble surface, respectively.

The kinematic boundary condition holds on S. We assume that the ratio of surface diffusion to surface advection of surfactant is sufficiently small that surface diffusion can be neglected. This is the limit of an immobile surfactant, and, on regions of S that are surfactant-covered, the velocity field satisfies the no-slip boundary condition. In the steady state, this implies that, in terms of the velocity components,

$$\text{on } S: \begin{cases} u_r = 0 \text{ and } u_z = 0 & \text{when } \Gamma > 0, \\ u_r - R'u_z = 0 & \text{when } \Gamma = 0. \end{cases} \tag{2.10}$$

Two additional constraints are that the bubble volume and the total amount of surfactant on S are the same in both the strained and unstrained states, so that

$$\frac{4}{3}\pi a_0^3 = 2\pi\int_0^l R^2(z)\,\mathrm{d}z \tag{2.11}$$

and

$$4\pi a_0^2\Gamma_0 = 4\pi\int_0^l \Gamma(z)R(z)(1+R'^2)^{1/2}\,\mathrm{d}z. \tag{2.12}$$

Here, a_0 and Γ_0 are the bubble radius and uniform surfactant concentration in the unstrained spherical state, and l is the bubble half-length in the z-direction in the strained state as defined at (2.3).

The governing equations and boundary conditions are made non-dimensional by setting

$$\boldsymbol{x} = l\tilde{\boldsymbol{x}}, \quad R(z) = b\tilde{R}(\tilde{z}), \quad \boldsymbol{u} = Gl\tilde{\boldsymbol{u}}, \quad p = G\mu\tilde{p}, \quad \sigma = \sigma_0\tilde{\sigma}, \quad \Gamma = \Gamma_0\tilde{\Gamma}, \tag{2.13}$$

where a tilde denotes that a quantity is dimensionless. Thus, lengths are made dimensionless by the bubble's half-length l, except for the radial distance to the free surface which is made dimensionless by the radial distance b at $z=0$. Dimensionless groupings are defined by

$$\epsilon = \frac{b}{l}, \quad \nu = \frac{a_0}{l}, \quad \beta = \frac{RT\Gamma_0}{\sigma_0}, \quad Q = \frac{G\mu a_0}{\sigma_0}. \tag{2.14}$$

When tildes on dimensionless quantities are dropped, the bubble surface is

$$S : r = \epsilon R(z) \text{ with } R(0) = 1,\ R(1) = 0. \tag{2.15}$$

The governing equations and the condition at infinity are given by setting μ and G to one in their dimensional counterparts (2.1) and (2.2), and the linear relation between surfactant concentration and surface tension becomes

$$\sigma = 1 - \beta\Gamma. \tag{2.16}$$

The stress-balance boundary conditions on S become

$$\frac{2}{(1+\epsilon^2 R'^2)}\left(\epsilon R'\frac{\partial u_r}{\partial r} + (1-\epsilon^2 R'^2)^{\frac{1}{2}}\left(\frac{\partial u_r}{\partial z} + \frac{\partial u_z}{\partial r}\right) - \epsilon R'\frac{\partial u_z}{\partial z}\right) = \frac{-\nu}{Q}\frac{\sigma'}{(1+\epsilon^2 R'^2)^{1/2}}, \tag{2.17}$$

$$p_i - p_e + \frac{2}{(1+\epsilon^2 R'^2)}\left(\frac{\partial u_r}{\partial r} - \epsilon R'\left(\frac{\partial u_r}{\partial z} + \frac{\partial u_z}{\partial r}\right) + \epsilon^2 R'^2\frac{\partial u_z}{\partial z}\right) = \frac{\nu}{Q\epsilon}\frac{\sigma}{R(1+\epsilon^2 R'^2)^{1/2}}\left(1 - \frac{\epsilon^2 R R''}{(1+\epsilon^2 R'^2)}\right), \tag{2.18}$$

and the no-slip and kinematic boundary conditions become

$$\text{on } S : \begin{cases} u_r = 0 \text{ and } u_z = 0 & \text{when } \Gamma > 0, \\ u_r - \epsilon R' u_z = 0 & \text{when } \Gamma = 0. \end{cases} \tag{2.19}$$

The constraints on bubble volume and total surfactant are now

$$\frac{2\nu^3}{3\epsilon^2} = \int_0^1 R^2\,\mathrm{d}z \tag{2.20}$$

and

$$\frac{\nu^2}{\epsilon} = \int_0^1 \Gamma R(1+\epsilon^2 R'^2)^{1/2}\,\mathrm{d}z. \tag{2.21}$$

3. Steady-state solutions

The bubble causes a modification of the flow from the imposed state of uniaxial extension, which is given by introducing point forces or Stokeslets, with distribution $f\boldsymbol{e}_z$, and point mass sources, with distribution g, situated along the bubble axis $r = 0$, $z \in [-1+\delta, 1-\delta]$. In terms of these distributions,

$$u_r = -\tfrac{1}{2}r + r(I_{1,3}(f) + I_{0,3}(g)), \tag{3.1}$$

$$u_z = z + I_{0,1}(f) + I_{2,3}(f) + I_{1,3}(g), \tag{3.2}$$

$$p_e = 2I_{1,3}(f), \tag{3.3}$$

$$\text{where } I_{m,n}(\phi) = \int_{-1+\delta}^{1-\delta} \phi(\xi)\frac{(z-\xi)^m}{(r^2+(z-\xi)^2)^{n/2}}\,\mathrm{d}\xi. \tag{3.4}$$

The problem is now reduced to finding the free-surface position $S : r = \epsilon R(z)$, the Stokeslet and mass source distributions f and g, and the surfactant concentration Γ or equivalently, from (2.16), the surface tension σ. On surfactant-covered parts of S, $\Gamma > 0$ and the two no-slip boundary conditions and two stress-balance conditions provide four equations for these four unknowns. On surfactant-free parts of S, $\Gamma = 0$ and the two no-slip boundary conditions are replaced by the one kinematic

boundary condition, which together with the two stress-balance conditions provides three equations for the unknowns R, f and g.

The components of the velocity gradient are given by differentiating equations (3.1) and (3.2), and are

$$\frac{\partial u_r}{\partial r} = -\tfrac{1}{2} + I_{1,3}(f) - 3r^2 I_{1,5}(f) + I_{0,3}(g) - 3r^2 I_{0,5}(g), \tag{3.5}$$

$$\frac{\partial u_r}{\partial z} = r(I_{0,3}(f) - 3I_{2,5}(f) - 3I_{1,5}(g)), \tag{3.6}$$

$$\frac{\partial u_z}{\partial r} = -r(I_{0,3}(f) + 3I_{2,5}(f) + 3I_{1,5}(g)), \tag{3.7}$$

$$\frac{\partial u_z}{\partial z} = 1 + I_{1,3}(f) - 3I_{3,5}(f) + I_{0,3}(g) - 3I_{2,5}(g). \tag{3.8}$$

3.1. *The completely covered case*

The exact form of the no-slip boundary condition $u_z = 0$ on $r = \epsilon R$ is

$$z + I_{0,1}(f) + I_{2,3}(f) + I_{1,3}(g) = 0. \tag{3.9}$$

The expansion of the integrals $I_{m,n}(\cdot)$ as $r \to 0$ is outlined in the Appendix, from which we find that when the dominant part of each expansion is included, the boundary condition is approximated by

$$z + 2\left\{ f\left(2\ln\frac{1}{\epsilon} + \ln\frac{4(1-z^2)}{R^2} - 1 \right) + \int_{-1+\delta}^{1-\delta} \frac{f(\xi) - f(z)}{|z-\xi|}\,\mathrm{d}\xi + \cdots \right\}$$
$$- g'\left\{ 2\ln\frac{1}{\epsilon} + \cdots \right\} = 0. \tag{3.10}$$

Throughout, an ellipsis denotes terms that are smaller by an algebraic power of ϵ than the last term that precedes it. After scalings for f and g are found, the term $I_{1,3}(g)$ in g will be seen not to contribute to equation (3.10) to the order of calculation given here, which allows computation of the dominant part of the expansions for each unknown up to all integer powers of $\ln(1/\epsilon)$.

The no-slip boundary condition $u_r = 0$ on $r = \epsilon R$ is

$$-\tfrac{1}{2} + I_{1,3}(f) + I_{0,3}(g) = 0, \tag{3.11}$$

which, on expansion of the integrals $I_{1,3}(f)$ and $I_{0,3}(g)$ following the same procedure as above, is approximated by

$$-\tfrac{1}{2} + f\left\{ \frac{1}{1-z} - \frac{1}{1+z} + \cdots \right\} - f'\left\{ 2\ln\frac{1}{\epsilon} + \ln\frac{4(1-z^2)}{R^2} - 2 + \cdots \right\}$$
$$+ \int_{-1+\delta}^{1-\delta} \frac{z-\xi}{|z-\xi|^3}(f(\xi) - f(z) - (\xi - z)f'(z))\,\mathrm{d}\xi + \cdots + g\left\{ \frac{2}{\epsilon^2 R^2} + \cdots \right\} = 0. \tag{3.12}$$

Adding the derivative with respect to z of equation (3.10) to twice equation (3.12), we see that $g = O(\epsilon^2 f)$. Equation (3.10) then implies that $f = O(\ln^{-1}(1/\epsilon))$ and that the term $I_{1,3}(g) = O(\epsilon^2)$, which is of higher order and can be neglected. Also, at higher orders, the dominant part of the expansions for f, g and R recur at integer powers of $\ln(1/\epsilon)$. We therefore introduce order one quantities $\tilde{f}$, $\tilde{g}$, f_n, g_n and R_n such that

$$f = \frac{\tilde{f}}{\ln(1/\epsilon)} \text{ where } \tilde{f} = f_0 + \frac{f_1}{\ln(1/\epsilon)} + \cdots + \frac{f_n}{\ln^n(1/\epsilon)} + \cdots, \tag{3.13}$$

$$g = \frac{\epsilon^2 \tilde{g}}{\ln(1/\epsilon)} \text{ where } \tilde{g} = g_0 + \frac{g_1}{\ln(1/\epsilon)} + \cdots + \frac{g_n}{\ln^n(1/\epsilon)} + \cdots, \tag{3.14}$$

$$R = R_0 + \frac{R_1}{\ln(1/\epsilon)} + \cdots + \frac{R_n}{\ln^n(1/\epsilon)} + \cdots. \tag{3.15}$$

With the term $I_{1,3}(g)$ shown to be of sufficiently high order that it can be omitted, equation (3.10) determines the expansion of f to all integer powers of $\ln(1/\epsilon)$, and its leading term is such that

$$f_0 = -\frac{1}{4}z. \tag{3.16}$$

The combination of the derivative of equation (3.10) with equation (3.12) that was formed earlier can be simplified, so that (3.12) can be replaced with

$$g = \frac{\epsilon^2}{2}\frac{\mathrm{d}}{\mathrm{d}z}(R^2 f), \tag{3.17}$$

which holds to all integer powers of $\ln(1/\epsilon)$.

In the tangential stress-balance equation (2.17), we estimate each term in the velocity gradient from (3.5) to (3.8) using the above scalings for f and g and the expansion of the integrals $I_{m,n}(\cdot)$ described in the Appendix. This shows first that (2.17) can be approximated by

$$\frac{\partial u_r}{\partial z} + \frac{\partial u_z}{\partial r} = \frac{-\nu}{Q}\frac{\mathrm{d}\sigma}{\mathrm{d}z}, \tag{3.18}$$

where the velocity gradient terms sum to $-6\epsilon R(I_{2,5}(f) + I_{1,5}(g))$. Of these, the integral $I_{1,5}(g)$ is of higher order and can be neglected, and the approximation of the integral $I_{2,5}(f)$ is such that the tangential stress balance simplifies to

$$\frac{4f}{\epsilon R} = \frac{\nu}{Q}\frac{\mathrm{d}\sigma}{\mathrm{d}z}, \tag{3.19}$$

which holds to all integer powers of $\ln(1/\epsilon)$. Since σ and its derivative are both of order one, the scaling (3.13) for f shows that $\nu/Q = O(1/\epsilon \ln(1/\epsilon))$.

We now estimate terms in the normal stress-balance equation (2.18). The exterior pressure $p_e = 2I_{1,3}(f)$ from equation (3.3), so that the expansion of $I_{1,3}(f)$ and scaling of f imply that p_e is of order one. Each term in the velocity gradient is found from (3.5) to (3.8) to be at most of order $O(1/\ln(1/\epsilon))$. The surface tension term on the right-hand side of (2.18) is known from the estimate of ν/Q above to be of order $O(1/\epsilon^2 \ln(1/\epsilon))$; it is therefore dominant and is balanced by the internal pressure p_i. The normal stress-balance equation therefore simplifies to

$$p_i = \frac{\nu}{Q\epsilon}\frac{\sigma}{R}, \tag{3.20}$$

which holds to all integer powers of $\ln(1/\epsilon)$.

Based on these estimates of the stress balance at the drop surface, we introduce order-one quantities $\tilde{p}_i$, p_{in}, σ_n and Λ defined by

$$p_i = \frac{\tilde{p}_i}{\epsilon^2 \ln(1/\epsilon)} \text{ where } \tilde{p}_i = p_{i0} + \frac{p_{i1}}{\ln(1/\epsilon)} + \cdots + \frac{p_{in}}{\ln^n(1/\epsilon)} + \cdots, \tag{3.21}$$

$$\sigma = \sigma_0 + \frac{\sigma_1}{\ln(1/\epsilon)} + \cdots + \frac{\sigma_n}{\ln^n(1/\epsilon)} + \cdots, \tag{3.22}$$

$$\frac{\nu}{Q} = \frac{1}{\epsilon \ln(1/\epsilon)\Lambda}. \tag{3.23}$$

The parameter Λ is a scaled capillary number. Written in terms of these order-one quantities, the two stress-balance equations are

$$\frac{\mathrm{d}\sigma}{\mathrm{d}z} = \frac{4\Lambda \tilde{f}}{R}, \quad \sigma = \Lambda \tilde{p}_i R, \tag{3.24a, b}$$

and hold to all integer powers of $\ln(1/\epsilon)$.

Since the fluid inside the bubble is inviscid and at rest, the interior pressure p_i is constant, i.e. independent of z, from which (3.24*b*) shows that the surface tension σ and the bubble radius R are equal up to a multiplicative constant. However, from the boundary condition (2.15), $R=0$ at the bubble endpoint $z=1$, which implies that σ is also zero there. Since the surface tension cannot truly vanish, we anticipate that there is a non-uniformity in the expansions near the endpoints of the bubble, $z=\pm 1$. We return to this in § 4.

On eliminating σ between (3.24*a*) and (3.24*b*), we find a single first-order differential equation for R in terms of the scaled Stokeslet distribution and internal pressure, that is

$$\frac{\mathrm{d}}{\mathrm{d}z} R^2 = \frac{8\tilde{f}}{\tilde{p}_i}, \tag{3.25}$$

which is subject to the two boundary conditions,

$$R(0) = 1, \quad R(1) = 0, \tag{3.26}$$

of (2.15), to all integer powers of $\ln(1/\epsilon)$. At leading order, since $\tilde{f} = f_0 = -z/4$ from (3.16) and $\tilde{p}_i = p_{i0}$ from (3.21), equation (3.25) becomes $(\mathrm{d}/\mathrm{d}z)R_0^2 = -2z/p_{i0}$. Integrating this with respect to z and applying the leading-order boundary conditions $R_0(0)=1$ and $R_0(1)=0$, we find that

$$R_0 = (1-z^2)^{1/2}, \quad p_{i0} = 1. \tag{3.27}$$

At higher orders, the solution procedure is to find f_n from equation (3.10) (with the term in g omitted), and then to find R_n and p_{in} by integrating equation (3.25) with the boundary conditions (3.26). Expressions for g_n and σ_n are then found from (3.17) and (3.24*b*). Specifically, substituting the solution for R_0 of (3.27) in equation (3.10), we find that

$$2f_1 + f_0(2\ln 2 - 1) + \int_{-1}^{1} \frac{f_0(\xi) - f_0(z)}{|z-\xi|}\,\mathrm{d}\xi = 0, \tag{3.28}$$

and, since $f_0 = -z/4$,

$$f_1 = -\tfrac{1}{4}\alpha z \quad \text{where} \quad \alpha = \tfrac{3}{2} - \ln 2. \tag{3.29}$$

Equation (3.25), together with the expansions (3.13), (3.15) and (3.21) and the solutions for f, R, and p_{in} at previous orders, becomes

$$\frac{\mathrm{d}}{\mathrm{d}z}(R_0 R_1) = (p_{i1} - \alpha)z, \tag{3.30}$$

so that on integrating with respect to z and applying the boundary conditions $R_0(0) = R_0(1) = 0$ implied by (3.26), we find that

$$R_1 = 0, \quad p_{i1} = \alpha. \tag{3.31}$$

It turns out that simple closed-form expressions for the solution can be found to all integer powers of $\ln(1/\epsilon)$, and that

$$f_k = -\frac{1}{4}\alpha^k z, \quad R_k = 0, \quad p_{ik} = \alpha^k \text{ for } k \geqslant 1, \tag{3.32}$$

as is shown by the following inductive argument. If (3.32) is valid for all integer k with $1 \leqslant k \leqslant n-1$ for some n, then equation (3.10) implies that a relation between f_{n-1} and f_n holds that is given by putting $f_0 \mapsto f_{n-1}$ and $f_1 \mapsto f_n$ in (3.28). Hence, $f_n = -\alpha^n z/4$. From (3.32), the first n terms of the expansion (3.21) for $\tilde{p}_i$ form a geometric series, the sum of which gives

$$\tilde{p}_i = \frac{1-(\alpha/\ln(1/\epsilon))^n}{1-\alpha/\ln(1/\epsilon)} + \frac{p_{in}}{\ln^n(1/\epsilon)} + O\big(\ln^{-(n+1)} 1/\epsilon\big),$$

hence

$$\frac{1}{\tilde{p}_i} = 1 - \frac{\alpha}{\ln(1/\epsilon)} - \frac{(p_{in}-\alpha^n)}{\ln^n(1/\epsilon)} + O\big(\ln^{-(n+1)} 1/\epsilon\big).$$

When this is combined with the assumption of (3.32) for the expansion of f, equation (3.25) implies that

$$\frac{\mathrm{d}}{\mathrm{d}z}(R_0 R_n) = (p_{in} - \alpha^n) z, \tag{3.33}$$

so that, on integrating with respect to z and applying the boundary conditions $R_n(0) = R_n(1) = 0$, we find that

$$R_n = 0, \quad p_{in} = \alpha^n, \tag{3.34}$$

and (3.32) is seen to hold. The expansion for σ follows from (3.24*b*) and the expansion for g follows from equation (3.17), which give $\sigma_n = \Lambda\alpha^n(1-z^2)^{1/2}$ and $g_n = \alpha^n(3z^2-1)/8$.

Each of the above expansions is a geometric series, and when summed these give the following solution to all integer powers of $\ln(1/\epsilon)$:

$$\left.\begin{aligned} f = \frac{-\alpha_\epsilon z}{4\ln(1/\epsilon)}, \quad g = \frac{\epsilon^2\alpha_\epsilon(3z^2-1)}{8\ln(1/\epsilon)}, \quad R = (1-z^2)^{1/2}, \\ \sigma = \Lambda\alpha_\epsilon(1-z^2)^{1/2}, \quad p_i = \frac{\alpha_\epsilon}{\epsilon^2\ln(1/\epsilon)}, \quad \text{where } \alpha_\epsilon = \frac{1}{1-\alpha/\ln(1/\epsilon)}. \end{aligned}\right\} \tag{3.35}$$

Once it is determined that the free surface $r = \epsilon R(z)$ is ellipsoidal, since it is a no-slip surface it is perhaps not surprising that the solution can be found to all orders of $\ln(1/\epsilon)$. This fact has previously been noted for a rigid slender ellipsoidal solid by Tillet (1970), and is consistent with the exact solution of Jeffery (1922) for a rigid ellipsoid of arbitrary aspect ratio. Here, we find the same ellipsoidal shape occurs fortuitously for an inviscid bubble covered with a non-uniform distribution of immobile surfactant (3.35).

The constraints for conservation of bubble volume and conservation of total surfactant can be evaluated to the same level of approximation. From the solution for R of (3.35), conservation of bubble volume (2.20) implies that ν and ϵ are related by

$$\nu = \epsilon^{2/3}. \tag{3.36}$$

Conservation of total surfactant (2.21), together with (3.36) and the relation $\sigma = 1-\beta\Gamma$ of (2.16), simplifies to become $\int_0^1 (1-\sigma) R\, dz = \beta\epsilon^{1/3}$ to all integer powers of $\ln(1/\epsilon)$. From the solutions for R and σ of (3.35) together with expressions (3.23) and (3.36),

which give the scaled capillary number Λ in terms of ϵ and Q, we find that the capillary number Q is given in terms of the aspect ratio ϵ and the parameter β by

$$Q = \tfrac{3}{2}\epsilon^{5/3}\ln(1/\epsilon)\left(1 - \frac{\alpha}{\ln(1/\epsilon)}\right)\left(\tfrac{1}{4}\pi - \beta\epsilon^{1/3}\right). \tag{3.37}$$

With increasing deformation, that is with decreasing aspect ratio ϵ, the monotone behaviour of the relation $\sigma = 1 - \beta\Gamma$ and of the solution (3.35) for σ in terms of z show that the surfactant concentration Γ first reaches zero at $z = 0$, when $\Lambda\alpha_\epsilon = 1$. In terms of β and ϵ, this occurs when

$$\beta\epsilon^{1/3} = \tfrac{1}{4}\pi - \tfrac{2}{3}. \tag{3.38}$$

With further increase of deformation, and thus smaller values of ϵ, a change in the solution occurs that is marked by the development of a surfactant-free or clean, central part of the bubble centred on $z = 0$, accompanied by stagnant surfactant-caps in a neighbourhood of the bubble endpoints $z = \pm 1$.

3.2. *The partly covered case*

In this case, the surfactant concentration Γ is identically zero on a central part of the bubble surface with $z \in (-a, a)$, and is positive elsewhere. As a consequence, the Stokeslet and mass source distributions f and g are denoted by

$$(f, g) = \begin{cases} (f^-, g^-), & z \in (-a, a), \\ (f^+, g^+), & z \in (-1+\delta, -a) \cup (a, 1-\delta), \end{cases} \tag{3.39}$$

where f and g may be discontinuous at $z = \pm a$. Other unknowns such as the bubble surface are still denoted by the same variable names as in the completely covered case for all z. It turns out that in this section we construct 'outer' solutions for f, g, R and σ, in the sense that the expansions are sought in the limit where z is fixed as $\epsilon \to 0$. In addition to a non-uniformity that can be expected, based on the analysis of the completely covered case, to occur near the bubble endpoints, we find that there is an additional non-uniformity of the outer expansions in a neighbourhood of $z = a$. This neighbourhood is small in the limit $\epsilon \to 0$, and the 'stick–slip' problem that is required to resolve the solution locally is not investigated here.

Since the solution is expected to be continuous with respect to the parameter a in the limit $a \to 0$, the scalings for f^+, g^+ and p_i with respect to ϵ are taken to be the same as the scalings for f, g and p_i in the completely covered case, that is

$$f^+ = \frac{\tilde{f}^+}{\ln(1/\epsilon)}, \quad g^+ = \frac{\epsilon^2\tilde{g}^+}{\ln(1/\epsilon)}, \quad p_i = \frac{\tilde{p}_i}{\epsilon^2\ln(1/\epsilon)}. \tag{3.40}$$

The variables with tildes, together with R and σ, are of order one and have expansions in integer powers of $\ln(1/\epsilon)$, e.g.

$$f^+ = \frac{\tilde{f}^+}{\ln(1/\epsilon)} \text{ where } \tilde{f}^+ = f_0^+ + \frac{f_1^+}{\ln(1/\epsilon)} + \cdots + \frac{f_n^+}{\ln^n(1/\epsilon)} + \cdots, \tag{3.41}$$

$$R = R_0 + \frac{R_1}{\ln(1/\epsilon)} + \cdots + \frac{R_n}{\ln^n(1/\epsilon)} + \cdots. \tag{3.42}$$

We begin by seeking scalings for f^- and g^- when $z \in [0, a)$.

$z \in [0, a)$.

As in the completely covered case, the dominant balance of terms in equation (2.18) for continuity of normal stress is between the internal pressure p_i and the surface

tension, so that an equation analogous to (3.20) holds and is valid to all integer powers of $\ln(1/\epsilon)$. However, since $\Gamma = 0$ when $z \in [0, a)$ the surface tension σ is equal to unity. Next, since the scaling for p_i is unchanged, the scaling for ν/Q is also unchanged and is given by (3.23), namely $\nu/Q = 1/(\epsilon \ln(1/\epsilon)\Lambda)$. The normal stress balance can therefore be expressed by (3.24*b*) with $\sigma = 1$, that is,

$$\Lambda \tilde{p}_i R = 1, \tag{3.43}$$

which holds to all integer powers of $\ln(1/\epsilon)$. Recalling that Λ and $\tilde{p}_i$ are independent of z, it follows that R is also independent of z, so that from the boundary condition $R(0) = 1$ of (2.15) we have

$$R = 1, \quad \text{hence } \Lambda \tilde{p}_i = 1, \tag{3.44a, b}$$

to all integer powers of $\ln(1/\epsilon)$.

The result that $R = 1$ simplifies expression of the kinematic boundary condition, which to the same level of approximation becomes $u_r = 0$, and implies that, as in equation (3.11), $-1/2 + I_{1,3}(f) + I_{0,3}(g) = 0$. When dominant contributions from both f^- and g^- are included, the kinematic condition becomes

$$\begin{aligned} -\tfrac{1}{2} + f^- \left\{ \frac{1}{a-z} - \frac{1}{a+z} + \cdots \right\} - f^{-\prime} \left\{ 2\ln(1/\epsilon) + \ln \frac{4(a^2 - z^2)}{R^2} - 2 + \cdots \right\} \\ + \int_{-a}^{a} \frac{z-\xi}{|z-\xi|^3} (f^-(\xi) - f^-(z) - (\xi - z) f^{-\prime}(z)) \, \mathrm{d}\xi - \int_a^1 \frac{f^+(\xi)}{(\xi - z)^2} \, \mathrm{d}\xi \\ + \int_{-1}^{-a} \frac{f^+(\xi)}{(z-\xi)^2} \, \mathrm{d}\xi + \cdots + g^- \left\{ \frac{2}{\epsilon^2 R^2} + \cdots \right\} = 0. \end{aligned} \tag{3.45}$$

Here, the integral of the Stokeslet distribution $I_{1,3}(f)$ results in a total of three integral terms, one over the surfactant-free region $z \in (-a, a)$ and one over each of the two surfactant-caps, where the correction δ in the distribution endpoints is omitted since, as in the completely covered case, it turns out to be small like ϵ^2. Integrals over the surfactant-caps containing g^+ are also algebraically small in ϵ and can be neglected, since from (3.40), $g^+ = O(\epsilon^2/\ln(1/\epsilon))$.

Since the radius $R = 1$ and the surface tension $\sigma = 1$ are constant on the surfactant-free region, to the order of calculation required, the equation for continuity of tangential stress (2.17) reduces to $\partial_z u_r + \partial_r u_z = 0$, cf. (3.18). From the expressions (3.5) to (3.8) for the velocity gradient in terms of the Stokeslet and mass source distributions, this implies that $I_{2,5}(f) + I_{1,5}(g) = 0$, so that when dominant contributions from f^- and g^- are included we have

$$\frac{2}{3\epsilon^2 R^2} f^-(z) + \cdots + \int_a^1 \frac{f^+(\xi)}{(\xi - z)^3} \, \mathrm{d}\xi + \int_{-1}^{-a} \frac{f^+(\xi)}{(z-\xi)^3} \, \mathrm{d}\xi + \cdots - \frac{2}{3\epsilon^2 R^2} g^{-\prime} + \cdots = 0. \tag{3.46}$$

This contains integrals of the Stokeslet distribution over each of the two surfactant-caps, but other terms such as integrals of the Stokeslet distribution over the surfactant-free region and terms involving $g^\pm$ are found to be of higher order.

Recalling that $f^+ = O(1/\ln(1/\epsilon))$ from (3.40), we see that balancing a maximal number of terms in equation (3.46) implies that f^- and $g^{-\prime}$ are both of order $O(\epsilon^2/\ln(1/\epsilon))$. In equation (3.45), all terms in f^- are thus algebraically small and can be neglected, and g^- is of order ϵ^2. Further, since $R = 1$ to all integer powers of $\ln(1/\epsilon)$, at leading order, g^- is independent of z with $g^- = \epsilon^2/4$. Introducing order-one

quantities $\tilde{f}^-$, $\tilde{g}^-$, f_n^- and g_n^-, we therefore have

$$f^- = \frac{\epsilon^2 \tilde{f}^-}{\ln(1/\epsilon)} \text{ where } \tilde{f}^- = f_0^- + \frac{f_1^-}{\ln(1/\epsilon)} + \cdots + \frac{f_n^-}{\ln^n(1/\epsilon)} + \cdots, \tag{3.47}$$

$$g^- = \epsilon^2 \tilde{g}^- \text{ where } \tilde{g}^- = g_0^- + \frac{g_1^-}{\ln(1/\epsilon)} + \cdots + \frac{g_n^-}{\ln^n(1/\epsilon)} + \cdots, \tag{3.48}$$

$$g_0^- = \tfrac{1}{4}. \tag{3.49}$$

These scalings for f^- and g^-, together with the result that $R = 1$ to all integer powers of $\ln(1/\epsilon)$, imply that the kinematic boundary condition (3.45) simplifies to become

$$\tilde{g}^- = \tfrac{1}{4} + \frac{1}{2\ln(1/\epsilon)} \left(\int_a^1 \frac{\tilde{f}^+(\xi)}{(\xi - z)^2} \, \mathrm{d}\xi - \int_{-1}^{-a} \frac{\tilde{f}^+(\xi)}{(z - \xi)^2} \, \mathrm{d}\xi \right), \tag{3.50}$$

to all integer powers of $\ln(1/\epsilon)$, and gives g^- in terms of f^+. Also, on differentiating this equation with respect to z, the integrals of the Stokeslet distribution over the surfactant-caps can be eliminated from equation (3.46), and we find that

$$f^- = -\tfrac{1}{2} g^{-\prime}, \tag{3.51}$$

which gives f^- via g^- in terms of f^+ to all integer powers of $\ln(1/\epsilon)$.

Given the scalings (3.40) for f^+ and g^+, a search for different scalings for f^- and g^- that balances a subset of terms in equation (3.46) leads either to an inconsistency or to the scalings just found. These contrast with the scalings found by Buckmaster (1972) and Acrivos & Lo (1978) for a bubble that is completely free of surfactant and is situated in a flow with the same strain, for which $p_i = O(1/\epsilon)$ and f and g are both of order $O(\epsilon^2)$.

$z \in (a, 1)$.

The boundary conditions on the surfactant-caps lead to equations for f^+ and g^+ that parallel those already found in § 3.1 for f and g when a bubble is completely covered in surfactant.

The exact form of the no-slip boundary condition $u_z = 0$ is $z + I_{0,1}(f) + I_{2,3}(f) + I_{1,3}(g) = 0$, per (3.9). When the domain of integration for each integral is subdivided into surfactant-caps $z \in (-1, -a) \cup (a, 1)$ and the surfactant-free region $z \in (-a, a)$, the integrals $I_{0,1}(f)$ and $I_{2,3}(f)$ consist of an integral over $z \in (a, 1)$ that is singular as $r \to 0$ and has an expansion similar to that used in deriving equation (3.10), together with integrals over $z \in (-1, -a)$ and $z \in (-a, a)$ that are regular as $r \to 0$. From the known scalings of f^+ and f^-, the contribution from the surfactant-free region is found to be algebraically small in ϵ and can therefore be neglected, while the contributions from both surfactant-caps must be retained. When contributions to $I_{1,3}(g)$ are estimated in the same way, $I_{1,3}(g)$ is found to be algebraically small in ϵ, so that, as for the surfactant-covered bubble, it can be neglected. As a consequence, the boundary condition takes a form that resembles (3.10), namely,

$$z + 2\left\{ f^+\left(2\ln(1/\epsilon) + \ln \frac{4(z-a)(1-z)}{R^2} - 1 \right) + \int_a^1 \frac{f^+(\xi) - f^+(z)}{|z - \xi|} \, \mathrm{d}\xi + \int_{-1}^{-a} \frac{f^+(\xi)}{z - \xi} \, \mathrm{d}\xi + \cdots \right\} = 0, \tag{3.52}$$

which holds to all integer powers of $\ln(1/\epsilon)$.

Similar reasoning shows that the no-slip condition $u_r = 0$ can be expressed in a form resembling (3.12), as

$$-\tfrac{1}{2} + f^+\left\{\frac{1}{1-z} - \frac{1}{z-a}\right\} - f^{+\prime}\left\{2\ln(1/\epsilon) + \ln\frac{4(z-a)(1-z)}{R^2} - 2\right\} + \int_a^1 \frac{z-\xi}{|z-\xi|^3}(f^+(\xi) - f^+(z) - (\xi - z)f^{+\prime}(z))\,\mathrm{d}\xi + \int_{-1}^{-a} \frac{f^+(\xi)}{(z-\xi)^2}\,\mathrm{d}\xi + \cdots + g^+\left\{\frac{2}{\epsilon^2 R^2} + \cdots\right\} = 0 \tag{3.53}$$

to all integer powers of $\ln(1/\epsilon)$.

A simpler expression for g^+ is given by differentiating equation (3.52) with respect to z and adding twice equation (3.53), which gives

$$g^+ = \frac{\epsilon^2}{2}\frac{\mathrm{d}}{\mathrm{d}z}(R^2 f^+), \tag{3.54}$$

to all integer powers of $\ln(1/\epsilon)$. This is the same as equation (3.17) for a surfactant-covered bubble under $f \mapsto f^+$ and $g \mapsto g^+$.

In considering the continuity of stress boundary conditions when $z \in (a, 1)$, we find that the analogy between a completely surfactant-covered bubble and surfactant-caps on a partly surfactant-covered bubble is even more direct. In the completely covered case, the continuity of stress boundary conditions (2.17) and (2.18) reduce to equations (3.24*a*) and (3.24*b*), and on retracing this analysis for surfactant-caps, it is found in considering, for example, the right-hand cap $z \in (a, 1)$ that no contributions occur from the Stokeslet and mass source distributions on either the surfactant-free region or the left-hand cap. Further, no non-local or additional local contributions occur from the right-hand cap. As a consequence, equation (3.24*a*) is modified by putting $\tilde{f} \mapsto \tilde{f}^+$, and in equation (3.24*b*), since the pressure inside the bubble is independent of z and such that $\Lambda\tilde{p}_i = 1$ from (3.44), the continuity of stress boundary conditions reduce to

$$\frac{\mathrm{d}\sigma}{\mathrm{d}z} = \frac{4\Lambda\tilde{f}^+}{R}, \quad \sigma = R \tag{3.55}$$

to all integer powers of $\ln(1/\epsilon)$. When σ is eliminated, since $\Lambda\tilde{p}_i = 1$, the first equation can be written as

$$\frac{\mathrm{d}}{\mathrm{d}z}R^2 = \frac{8\tilde{f}^+}{\tilde{p}_i}. \tag{3.56}$$

The solution can now be constructed at successive powers of $\ln(1/\epsilon)$. At leading order, from equation (3.52),

$$f_0^+ = -\tfrac{1}{4}z. \tag{3.57}$$

When this is substituted in (3.56), the first-order equation for R_0 that results can readily be integrated with respect to z. The boundary conditions on R are that $R(1) = 0$ to all orders from (2.15), and a second boundary condition that, strictly, arises as $z \to a^+$ as a result of matching with the solution of the stick-slip problem in a neighbourhood of $z = a$. However, since the leading-order solution is to be continuous at $z = a$, $R_0(a) = 1$, and hence,

$$R_0 = \left(\frac{1-z^2}{1-a^2}\right)^{1/2}, \quad p_{i0} = 1 - a^2. \tag{3.58a, b}$$

From equation (3.54), it follows that

$$g_0^+ = \frac{3z^2-1}{8(1-a^2)}. \tag{3.59}$$

The solution at higher orders.

The solution for f_1^+ is given by equation (3.52) on substituting the leading-order solution (3.57) for f_0^+ and (3.58) for R_0, from which we have

$$f_1^+ = \tfrac{1}{8}\left(z\ln\frac{4(1-a^2)(z-a)}{(z+a)} + 2a - 3z\right). \tag{3.60}$$

This includes contributions due to the leading-order Stokeslet distribution over both surfactant-caps. A straightforward but lengthier calculation gives R_1 in terms of p_{i1} when equation (3.56) is integrated with respect to z with the one boundary condition $R_1(a)=0$. The other boundary condition $R_1(1)=0$ then determines an expression for the pressure p_{i1}, and we find that

$$R_1 = \frac{(z-a)}{4((1-z^2)(1-a^2))^{1/2}}\left((z+a)\ln\frac{(z-a)(1+a)}{(z+a)(1-a)} + 2a(1-z)\right), \tag{3.61}$$

$$p_{i1} = \tfrac{1}{2}(1-a)(3+a) - (1-a^2)\ln 2(1-a). \tag{3.62}$$

The relation (3.44*b*) together with (3.58*b*) determines $\Lambda_0 = 1/(1-a^2)$ and $\Lambda_1 = -p_{i1}/(1-a^2)^2$, where p_{i1} is given in (3.62).

The solution for g_1^+ is given by equation (3.54), and its computation is facilitated in the following way. Integration of equation (3.56) implies that $R^2 = (8/\tilde{p}_i)\int_1^z \tilde{f}^+(\xi)\,\mathrm{d}\xi$ to all integer powers of $\ln(1/\epsilon)$. Equation (3.54) can therefore be written as $\tilde{g}^+ = (2/\tilde{p}_i)(\mathrm{d}^2/\mathrm{d}z^2)(\int_1^z \tilde{f}^+\mathrm{d}\xi)^2$ to the same order, from which the solutions for f_0^+ and f_1^+ give

$$g_1^+ = \frac{1}{8(1-a^2)}\left(\frac{az(1+2a^2-3z^2)}{z^2-a^2} + \tfrac{1}{2}(1+a^2-6z^2)\ln\frac{4(1-a^2)(z-a)}{(z+a)}\right.$$
$$\left. + (3z^2-a^2)\ln 2(1-a) - \frac{(3+a)(3z^2-1)}{2(1+a)} + a - 3 - 3az + 9z^2\right). \tag{3.63}$$

We note that $f_1^+ \to -\alpha z/4$, $R_1 \to 0$, $p_{i1} \to \alpha$ and $g_1^+ \to \alpha(3z^2-1)/8$ as $a \to 0$, which is consistent with the solution (3.35) in the completely surfactant-covered case.

On the surfactant-free region $z \in [0, a)$, the solution for g_1^- is given by equation (3.50) on recalling that $f_0^+ = -z/4$. Hence

$$g_1^- = -\tfrac{1}{8}\ln\frac{1-z^2}{a^2-z^2} + \tfrac{1}{4}\left(\frac{1}{1-z^2} - \frac{a^2}{a^2-z^2}\right), \tag{3.64}$$

from which the solution for f_0^- follows from (3.51) as

$$f_0^- = -\tfrac{1}{8}z\left(\frac{1}{1-z^2} - \frac{1}{a^2-z^2}\right) - \tfrac{1}{4}z\left(\frac{1}{(1-z^2)^2} - \frac{a^2}{(a^2-z^2)^2}\right). \tag{3.65}$$

In principle, the expansions can be calculated at yet higher orders by continuing the sequence of steps outlined above. We note, however, that the integrals in equation (3.52) preclude the simple, closed-form expressions for the solution for f^+ that could be found to all integer powers of $\ln(1/\epsilon)$ for the completely surfactant-covered bubble. On the other hand, it is already clear from the orders given above that the expansions

have a non-uniformity at $z=a$, i.e. in a neighbourhood of the edge of the surfactant-cap. This is the neighbourhood of the stick–slip problem alluded to earlier, and to investigate it we must find the most singular part of $f^{\pm}$ as $z\to a$ to all integer powers of $\ln(1/\epsilon)$. This is discussed in the Appendix.

Although it is not possible to find a simple expression for f^{+} valid for general $O(1)$ values of $a>0$ to all integer powers of $\ln(1/\epsilon)$, such an expression can be found when a is algebraically small in ϵ. Further, there is an advantage to having such an expression when computing steady-state-solution branches: since the completely surfactant-covered solutions of the branch are computed to all orders of $\ln(1/\epsilon)$, a similar higher-order solution for partially covered bubbles leads to continuity at the transition point from partial to complete covering. We claim that in this limit, as $a\to 0$, the solution of equation (3.52) for f^{+} recovers the solution of equation (3.9) for f, that is $f^{+}=-\alpha_\epsilon z/(4\ln(1/\epsilon))$ where α_ϵ is defined in (3.35), and it is valid to all integers powers of $\ln(1/\epsilon)$ when a is algebraically small in ϵ, while we have shown above that it is valid to $O(1/\ln(1/\epsilon))$ for values of a that are $O(1)$. On integrating (3.56) and applying the boundary conditions $R(a)=1$ and $R(1)=0$, we then find that

$$R(z)=\left(\frac{1-z^2}{1-a^2}\right)^{1/2},\quad \tilde{p}_i=\alpha_\epsilon(1-a^2), \tag{3.66}$$

which is valid to all integer powers of $\ln(1/\epsilon)$ when a is algebraically small in ϵ, and to $O(1/\ln(1/\epsilon))$ at larger values of a. Since $\Lambda\tilde{p}_i=1$ to all orders of $\ln(1/\epsilon)$, it follows that

$$\Lambda=\frac{1}{\alpha_\epsilon(1-a^2)}, \tag{3.67}$$

to the same order of approximation as (3.66).

The constraints for conservation of bubble volume and conservation of total surfactant can be evaluated to the same order of approximation. Conservation of bubble volume (2.20) gives the relation

$$v=\epsilon^{2/3}\left(\frac{1+a+a^2}{1+a}\right)^{1/3}. \tag{3.68}$$

Conservation of total surfactant (2.21), together with (3.68) and the linear equation of state (2.16), simplifies to

$$\int_a^1 (1-R)R\,\mathrm{d}z=\beta\epsilon^{1/3}\left(\frac{1+a+a^2}{1+a}\right)^{2/3}, \tag{3.69}$$

where we have used $\sigma=R$, per (3.55), and the fact that $\Gamma=0$ for $z\in[0,a)$. The expression (3.69) provides a relation between a and ϵ, subject to the condition $\epsilon<(3\pi-8)^3/(12\beta)^3$ which is required by (3.38) for the partially covered case to hold. An expression for the capillary number Q in terms of ϵ and a now follows from (3.67), (3.68), and the relation $v/Q=1/(\epsilon\ln(1/\epsilon)\Lambda)$, viz.

$$Q=\epsilon^{5/3}\ln(1/\epsilon)\left(1-\frac{\alpha}{\ln(1/\epsilon)}\right)\frac{(1+a+a^2)^{1/3}}{(1-a^2)(1+a)^{1/3}}, \tag{3.70}$$

which is valid to all integer powers of $\ln(1/\epsilon)$ for a algebraically small in ϵ and to leading order for all a. Together, equations (3.69) and (3.70) provide a relation between the capillary number Q and the bubble slenderness ratio ϵ for the partly covered case. When a nonlinear equation of state is substituted for the linear one, the

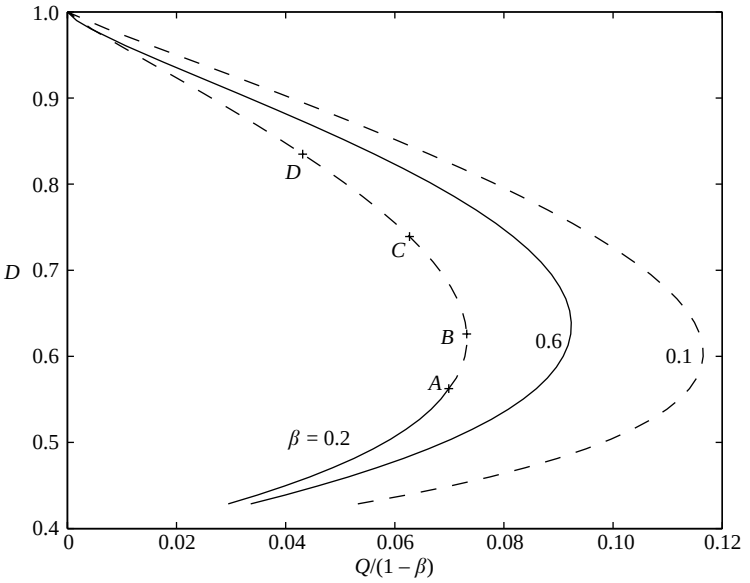

FIGURE 2. Steady-state response curves (D versus $Q^* = Q/(1-\beta)$) for a bubble with a linear equation of state. Curves are shown for $\beta = 0.1, 0.2, 0.6$. Solid curves represent completely surfactant-covered bubbles and dashed curves represent steady bubbles with stagnant surfactant-caps. Capital letters mark the locations of the plots in figure 3.

relation between a and ϵ of equation (3.69) is modified while equation (3.70) remains unchanged.

3.3. *Steady-state response*

In order to characterize the steady-state shapes, we introduce the deformation parameter

$$D = \frac{1-\epsilon}{1+\epsilon},$$

and a rescaled capillary number $Q^* = Q/(1-\beta)$, following Stone & Leal (1990), which is based on the equilibrium tension $\sigma_0(1-\beta)$ instead of the clean surface tension σ_0. Figure 2 shows the response curves for D versus Q^* for three representative values of β. A solid line denotes completely surfactant-covered bubbles, for which (3.37) holds, while a dashed line, described by (3.70), is associated with partially covered 'stagnant-cap' bubbles. The bubble shapes associated with locations $A-D$ on the $\beta = 0.2$ response curve are depicted in figure 3. The top bubble in the figure is completely covered with surfactant, while the lower three are stagnant-cap bubbles, with the location of the cap edge denoted by '+' markers.

Unlike the solution branches in the clean bubble case (Buckmaster 1972), for which steady states exist for arbitrarily large capillary number, our solutions exhibit a critical capillary number Q_c which depends on β, above which steady solutions no longer exist. Each response curve shows that there are two steady-state solutions for a given value of Q satisfying $Q < Q_c$. In related free-surface flow problems, e.g. drop deformation in a clean fluid system with viscosity ratio $\lambda = \mu_i/\mu > 0$ (Acrivos & Lo 1978), or steady bubbles with surfactant in an extensional Stokes flow that is two-dimensional (Siegel 1999), the turning point corresponds to a change in stability; the lower-branch solutions are stable steady states, whereas the upper-branch solutions

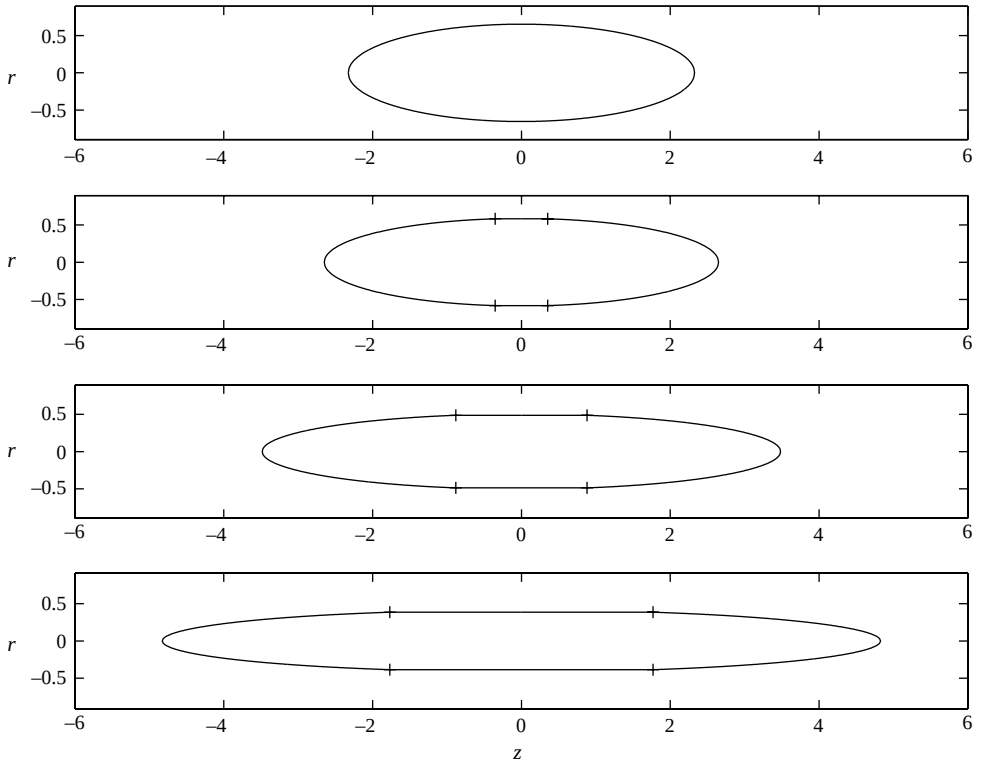

FIGURE 3. Steady profiles at capillary number marked by points $A-D$ on the $\beta=0.2$ response curve. These are shapes predicted to be observed in physical space, and the equivalent unstrained spherical bubble of the same volume has radius 1 and constant surfactant concentration $\Gamma=1$. The edges of the stagnant caps are indicated by '+' markers.

are unstable. This is most probably the case here, although we do not investigate stability of the solution branches. The turning point Q_c represents the maximum possible strain rate for which the bubble will advance to a steady state – for $Q > Q_c$ the bubble will burst. Time-dependent slender-bubble solutions, presented in § 5, show that the unsteady dynamics exhibit tip-streaming for $Q > Q_c$.

A plot illustrating the critical capillary number Q_c^* for bursting as a function of β is given in figure 4. Shown for comparison are values of Q_c^* computed by Stone & Leal (1990) via boundary integral numerical simulations of the evolution of a time-evolving bubble. The results of Stone & Leal (top two curves in the figure) are for viscosity ratio $\lambda=1.0$, and incorporate non-zero surface diffusion of surfactant, quantified via the dimensionless parameter $\gamma=\sigma_0(1-\beta)a/(\mu D_s)$. Our results correspond to $\lambda=0$ and $\gamma=\infty$ (lower curve). Despite the different parameter values, the curves show similarities in the magnitude of the critical capillary number and its variation with β. Further numerical simulations of Milliken *et al.* (1993) indicate that the critical capillary number Q_c^* is insensitive to the value of λ in the range $0.1-10$ for $\beta=0.3$ and $\gamma=1000$ (sensitivity to λ at this value of γ for other β was not considered). Our asymptotic results suggest that for negligible surface diffusion, this insensitivity should hold for $\beta \gtrsim 0.3$, because the lower-branch of steady (stable) bubble solutions are completely surfactant-covered in this range of β and the bubble surface is stagnant, so that the effect of the interior fluid is minimized. In contrast, for $\beta \lesssim 0.3$, there are

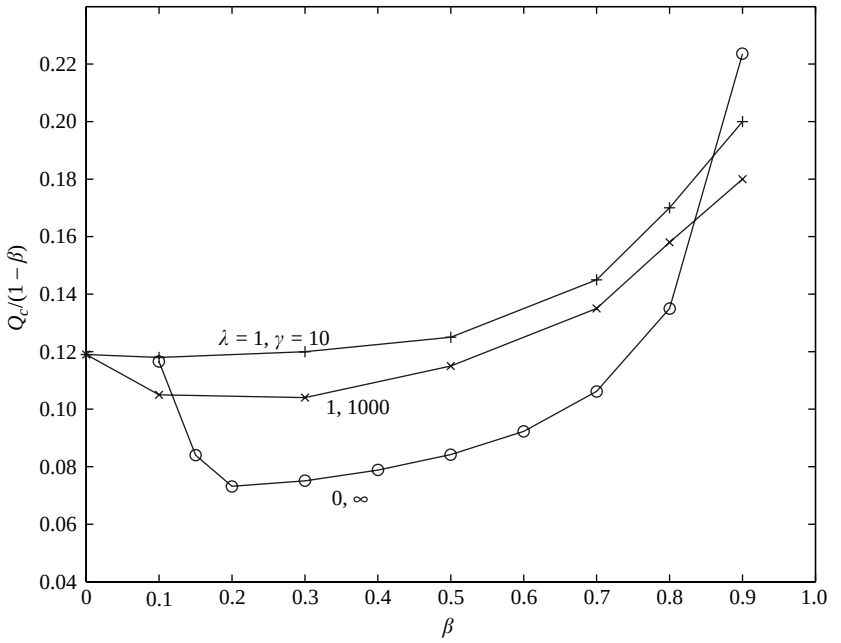

FIGURE 4. The critical capillary number $Q_c^* = Q_c/(1-\beta)$ as a function of β. The top two curves are from Stone & Leal (1990), and are for a viscosity ratio $\lambda = 1$ and surface diffusion $\gamma = 10$ and 1000. The lower curve shows our asymptotic result for $\lambda = 0$ and $\gamma = \infty$.

partially covered steady solutions on the lower-branch of the response curve, for which only the bubble end-caps are stagnant, so that the interior fluid can have a significant effect on bubble deformation and response. For this range of β, Q_c^* should be sensitive to variations in λ.

Surface diffusion of surfactant can have an effect on the critical capillary number, as shown in the figure. Decreasing the surface diffusion reduces the slip in surfactant-covered regions towards zero, and typically decreases the critical capillary number for a given surfactant concentration. The trend shown in the figure suggests that the agreement between our asymptotic results and the results of numerical simulation should be even better for yet larger γ. The physical consequences of other variations in parameters are discussed in Stone & Leal (1990) and Milliken *et al.* (1993).

The steady-solution branches for the nonlinear equation of state (2.6) are qualitatively the same as in figure 2. It is instructive to compare the critical capillary number Q_c for bursting as determined by our analysis, with the results found via numerical simulation of a time-evolving bubble (Eggleton *et al.* 2001) and by experiment (Hu, Pine & Leal 2000) for the nonlinear equation of state. To do so, define Γ_{eq} to be the uniform surfactant concentration on an unstrained spherical bubble with radius a and surface tension σ_{eq}, and introduce the parameters $x = \Gamma_{eq}/\Gamma_\infty$ and the elasticity number $E = RT\Gamma_\infty/\sigma_{eq}$. Then x is a measure of the total amount of surfactant on the bubble surface, and σ_{eq}/σ_0 is a monotone decreasing function of x, since from (2.6) they are related by $\sigma_{eq}/\sigma_0 = (1 - E\ln(1-x))^{-1}$. Figure 5 shows the dependence of a rescaled critical capillary number $Q_c\sigma_0/\sigma_{eq}$ on σ_{eq}/σ_0 for fixed $E = 0.2$, following Eggleton *et al.* (2001). The bottom curve is from the numerical

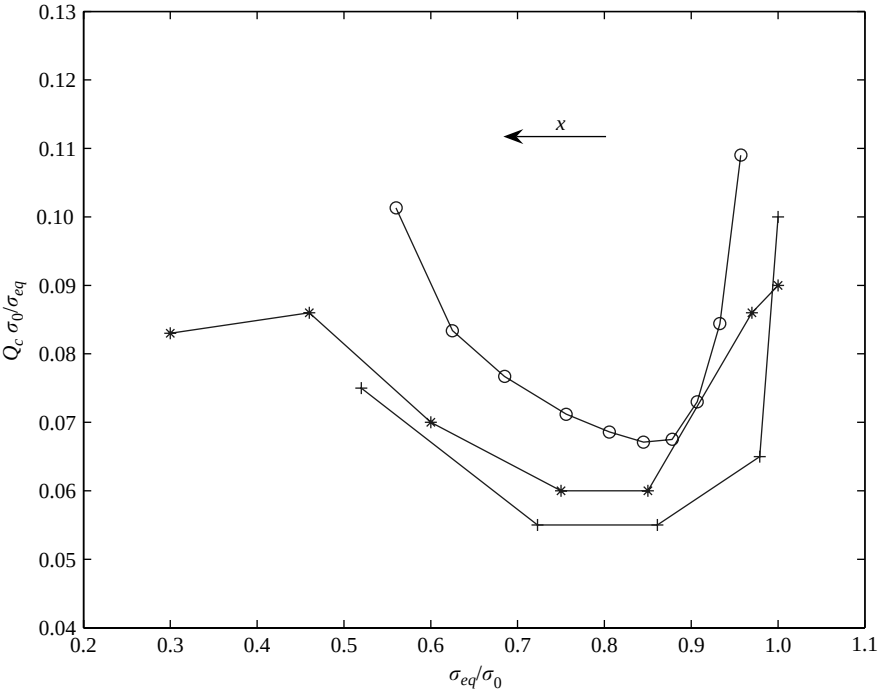

FIGURE 5. Comparison of the critical capillary number $Q_c\sigma_0/\sigma_{eq}$ (following Eggleton *et al.* 2001) for bursting. (o) Asymptotic theory, $\lambda = 0$; (*) experiment (Hu *et al.* 2000), $\lambda = 0.1$; (+) simulation (Eggleton *et al.* 2001), $\lambda = 0.05$. The direction of increasing $x = \Gamma_{eq}/\Gamma_0$ is shown in the figure.

simulations of Eggleton *et al.* (2001)†, computed using a boundary integral method with viscosity ratio $\lambda = 0.05$ and surface diffusion parameter $Pe_0 = \sigma_{eq}a/(\mu D_s)$ set at $10^3\sigma_0/\sigma_{eq}$. The middle curve is from the experiments of Hu *et al.* (2000) on drops with $\lambda = 0.1$, as presented in Eggleton *et al.* (2001). The upper curve is from our asymptotic theory with $\lambda = 0$ and $Pe_0 = \infty$. The curves show close correspondence in the magnitude of the critical capillary number and its variation with σ_{eq}/σ_0 despite the different values of λ and Pe_0. The physical significance of the non-monotone dependence of critical capillary number on σ_{eq}/σ_0 is discussed in Eggleton *et al.* (2001) and, for drops of unity viscosity ratio, in Eggleton, Pawar & Stebe (1999).

4. Steady-state solutions near an endpoint

We noted that the expansions constructed in § 3 predict a vanishing or zero surface tension at the bubble endpoints, so that they lose validity there. Also, near a rounded endpoint, the assumption that the surface shape R' is bounded no longer holds. The source of the non-uniformity can be traced to the expansion of the integrals $I_{m,n}(\phi)$, which were defined at (3.4), over the source distributions $\phi = f$ and $\phi = g$, and more specifically to the fact that the expansion of the functions $w_{m,n}(r, z)$ introduced in the Appendix differs, depending on whether the field point approaches the source distribution away from its endpoints or near an endpoint.

† An error in the abscissa locations of the curve points has been corrected.

Near the distribution and away from its endpoints, derivatives of $w_{m,n}(r, z)$ in the axial or z-direction, i.e. in the direction parallel to the distribution axis, are of order one, while r-derivatives are large, whereas in a neighbourhood of an endpoint, derivatives with respect to both r and z are large.

The solution in a neighbourhood of the endpoint $z = 1$ is readdressed by introducing a local coordinate for z and observing the expansion of the functions $w_{m,n}(r, z)$ as $r \to 0$ and $z \to 1$. We introduce a local coordinate η and a rescaling for the bubble surface, defined by

$$z = 1 - \delta + \epsilon^2 \eta, \quad r = \epsilon^2 \hat{R}(\eta), \tag{4.1}$$

so that $R(z) = \epsilon \hat{R}(\eta)$. The scalings for the interior pressure p_i and capillary number ratio ν/Q are as above at equations (3.21) and (3.23). The scalings for the source distributions f and g are those of the surfactant-covered regions, at equations (3.13), (3.14) and (3.40), while a rescaling for the surface tension $\sigma(z) = \epsilon \hat{\sigma}(\eta)$ is suggested by the behaviour of $\sigma(z)$ as $z \to 1$. We therefore put

$$p_i = \frac{\hat{p}_i}{\epsilon^2 \ln(1/\epsilon)}, \quad \frac{\nu}{Q} = \frac{1}{\epsilon \ln(1/\epsilon) \Lambda}, \quad f = \frac{\hat{f}}{\ln(1/\epsilon)}, \quad g = \frac{\epsilon^2 \hat{g}}{\ln(1/\epsilon)}, \quad \sigma = \epsilon \hat{\sigma}, \tag{4.2}$$

where rescaled quantities are all of order one and have expansions in integer powers of $\ln(1/\epsilon)$, e.g.

$$\hat{f} = \hat{f}_0 + \frac{\hat{f}_1}{\ln(1/\epsilon)} + \cdots. \tag{4.3}$$

Since the fluid in the bubble interior is inviscid, the interior pressure is independent of z and equal to the value found earlier in equation (3.27) when $a = 0$ and in equation (3.58*b*) when $a > 0$, that is

$$\hat{p}_{i0} = 1 - a^2 \tag{4.4}$$

for all a. Expansion of the integrals $I_{m,n}(\phi)$ now follows the method described in the Appendix, but where the source distributions f and g are expanded in Taylor series about the endpoint location $z = 1$.

The no-slip boundary condition $u_r = 0$ is given by equation (3.11), and at leading order in its local expansion, terms of $I_{1,3}(f)$ and $I_{0,3}(g)$ balance at order $O(1/\epsilon^2 \ln(1/\epsilon))$ to give

$$\frac{\hat{f}_0(1)}{\left(\eta^2 + \hat{R}_0^2\right)^{1/2}} + \frac{\hat{g}_0(1)}{\hat{R}_0^2}\left(1 - \frac{\eta}{\left(\eta^2 + \hat{R}_0^2\right)^{1/2}}\right) = 0. \tag{4.5}$$

In the no-slip boundary condition $u_z = 0$ of equation (3.9), terms of $I_{0,1}(f)$ and $I_{2,3}(f)$ balance at order $O(1)$ to give

$$\hat{f}_0(1) = -\tfrac{1}{4}. \tag{4.6}$$

This is the same as the values of both f_0 and f_0^+ of equations (3.16) and (3.57) as $z \to 1$. When (4.6) is substituted into equation (4.5), we find that the bubble surface in a neighbourhood of the endpoint is the paraboloid

$$\hat{R}_0^2 = \alpha_c^2 - 2\alpha_c \eta, \tag{4.7}$$

where the parameter $\alpha_c = 4\hat{g}_0(1)$. At equation (4.11) this is seen to take the value $\alpha_c = (1 - a^2)^{-1}$, and as a consequence $\hat{g}_0(1)$ is the same as both g_0 when $a = 0$ and g_0^+ when $a > 0$ as $z \to 1$, from equations (3.35) and (3.59). It also ensures that $\hat{R}_0$ matches as $\eta \to -\infty$ with the ellipsoids R_0 of equation (3.27) for the surfactant-covered bubble ($a = 0$) and of equation (3.58*a*, *b*) for the partially covered bubble ($a > 0$) as $z \to 1$.

In terms of the local variables of (4.1) and (4.2), but before expansion of the integrals $I_{m,n}(\phi)$ that give p_e and the components of the rate of strain tensor, the stress-balance boundary conditions on the bubble surface (2.17) and (2.18)become

$$\frac{2}{\left(1+\hat{R}_\eta^2\right)}\left(\hat{R}_\eta\frac{\partial u_r}{\partial r}+\left(1-\hat{R}_\eta^2\right)\tfrac{1}{2}\left(\frac{\partial u_r}{\partial z}+\frac{\partial u_z}{\partial r}\right)-\hat{R}_\eta\frac{\partial u_z}{\partial z}\right)=\frac{-1}{\epsilon^2\ln(1/\epsilon)\Lambda}\frac{\hat{\sigma}_\eta}{\left(1+\hat{R}_\eta^2\right)^{1/2}}, \tag{4.8}$$

$$\frac{\hat{p}_i}{\epsilon^2\ln(1/\epsilon)}-p_e+\frac{2}{\left(1+\hat{R}_\eta^2\right)}\left(\frac{\partial u_r}{\partial r}-\hat{R}_\eta\left(\frac{\partial u_r}{\partial z}+\frac{\partial u_z}{\partial r}\right)+\hat{R}_\eta^2\frac{\partial u_z}{\partial z}\right)$$
$$=\frac{1}{\epsilon^2\ln(1/\epsilon)\Lambda}\frac{\hat{\sigma}}{\hat{R}\left(1+\hat{R}_\eta^2\right)^{1/2}}\left(1-\frac{\hat{R}\hat{R}_{\eta\eta}}{\left(1+\hat{R}_\eta^2\right)}\right), \tag{4.9}$$

where an η-subscript denotes the derivative. Then, from equations (3.3) and (3.5) to (3.8), expansion of the integrals $I_{m,n}(\phi)$ together with the expression (4.7) for the known form of $\hat{R}_0$ gives the leading-order result that

$$p_e=\frac{-1}{2\epsilon^2\ln(1/\epsilon)\left(\eta^2+\hat{R}_0^2\right)^{1/2}},$$
$$\left(\frac{\partial u_r}{\partial r},\tfrac{1}{2}\left(\frac{\partial u_r}{\partial z}+\frac{\partial u_z}{\partial r}\right),\frac{\partial u_z}{\partial z}\right)=\frac{1}{4\alpha_c\epsilon^2\ln(1/\epsilon)}\frac{\hat{R}_0}{\eta^2+\hat{R}_0^2}(-\hat{R}_0,-\eta,\hat{R}_0).$$

When these are substituted in the tangential and normal components of the stress-balance boundary conditions, further use of (4.7) gives

$$\hat{\sigma}_0=\Lambda(2\alpha_c(\alpha_c-\eta))^{1/2}\left(\frac{2\hat{p}_{i0}(\alpha_c-\eta)+1}{3\alpha_c-2\eta}\right),\quad \frac{\mathrm{d}\hat{\sigma}_0}{\mathrm{d}\eta}=\frac{-\Lambda}{(2\alpha_c(\alpha_c-\eta))^{1/2}}. \tag{4.10}$$

These last two relations for $\hat{\sigma}_0$ are consistent only if $\hat{p}_{i0}\alpha_c=1$, and then from the expresssion (4.4) for $\hat{p}_{i0}$ we find

$$\hat{\sigma}_0=\Lambda(2(1-(1-a^2)\eta))^{1/2},\quad \alpha_c=(1-a^2)^{-1}. \tag{4.11}$$

The expansion of the surface tension σ that (4.11) provides matches as $\eta\to-\infty$ with that of (3.35) when $a=0$ and of (3.55) and (3.58) when $a>0$ as $z\to1$. It also provides a uniformly positive leading-order expression for the surface tension over the bubble surface, including the endpoints, at which $\sigma=\epsilon\Lambda$. Finally, since $z=1$ and $R=0$ at the endpoint, (4.1) and (4.7) give the leading-order estimate for δ, that

$$\delta=\frac{\epsilon^2}{2(1-a^2)}+\cdots. \tag{4.12}$$

5. Unsteady evolution

5.1. *Governing equations*

The equations governing the unsteady evolution of a slender axisymmetric bubble with insoluble surfactant at the interface are derived in this section. The bubble length l is now time-dependent, so it is convenient to non-dimensionalize lengths by l_0, defined as the half-length of the initial bubble shape. Other variables are made

non-dimensional as in (2.13), but with l replaced by l_0 and b by b_0, the initial half-width; dimensionless groupings are given by (2.14) after the same substitution. Define the non-dimensional length

$$L(t) = \frac{l}{l_0},$$

and note that $L(0) = 1$. The constraints on bubble volume (2.20) and surfactant concentration (2.21) are now

$$\frac{2\nu^3}{3\epsilon^2} = \int_0^{L(t)} R^2 \mathrm{d}z \tag{5.1}$$

and

$$\frac{\nu^2}{\epsilon} = \int_0^{L(t)} \Gamma R \sqrt{(1+\epsilon^2 R'^2)}\, \mathrm{d}z. \tag{5.2}$$

At the interface $r = \epsilon R(z)$, the stress-balance conditions (2.17) and (2.18) still hold and are supplemented by the kinematic condition, which takes the non-dimensional form

$$u_r = \epsilon \frac{\partial R}{\partial t} + \epsilon R' u_z, \tag{5.3}$$

where time has been non-dimensionalized by G^{-1}. An equation for the evolution of surfactant concentration Γ is derived in coordinate-free form in Wong, Rumschitzki & Maldarelli (1996), and in cylindrical coordinates, its non-dimensional form is

$$\frac{\partial \Gamma}{\partial t} + \frac{1}{R(1+\epsilon^2 R'^2)^{1/2}} \frac{\partial}{\partial z}\left[\frac{R\Gamma}{(1+\epsilon^2 R'^2)^{1/2}}(\epsilon u_r R' + u_z)\right] - \frac{\epsilon^2 R'}{1+\epsilon^2 R'^2} \frac{\partial R}{\partial t} \frac{\partial \Gamma}{\partial z} + \frac{\Gamma(u_r - \epsilon R' u_z)}{\epsilon R(1+\epsilon^2 R'^2)}\left[1 - \frac{\epsilon^2 R R''}{1+\epsilon^2 R'^2}\right] = 0, \tag{5.4}$$

where a prime denotes the derivative with respect to z. Here, we have assumed the limiting case in which the surface Péclet number, defined by $Pe = G l_0^2 / D$ with surface diffusivity D, tends to infinity, so that surface diffusion is negligible compared with surface transport.

As in the steady state, the flow exterior to the bubble is described by introducing Stokelets and point mass sources on the bubble axis $z \in [-L + \delta, L - \delta]$, where δ is time-dependent. The components of velocity and pressure are given in equations (3.1)–(3.3), while expressions for the velocity gradient are given in equations (3.5)–(3.8). The boundary conditions are approximated by expanding the integrals $I_{m,n}(\cdot)$ as $r \to 0$ and keeping the dominant part of each expansion, in a way similar to that for constructing the steady solutions of § 3. To leading order in f and g, the tangential stress balance (2.17) has the form

$$3\epsilon R' - \frac{4(g'R - R'g)}{\epsilon R^2} + \frac{4f}{\epsilon R} + \cdots = \frac{\nu}{Q}\sigma', \tag{5.5}$$

while the normal stress balance (2.18) at leading order is

$$p_i - 1 - \frac{4g}{\epsilon^2 R^2} + \frac{4R'f}{R} + \cdots = \frac{\nu}{Q\epsilon}\frac{\sigma}{R}. \tag{5.6}$$

The kinematic condition (5.3) at leading order is given by

$$R_t + zR' = -(2f'R + 4fR')\ln(1/\epsilon) + \frac{2g}{\epsilon^2 R} - \frac{R}{2} + \cdots. \tag{5.7}$$

In each of the above equations, an ellipsis denotes terms in f and g that are smaller than those kept by a factor of at least $\epsilon \ln 1/\epsilon$.

A scaling that is consistent with the above equations is $g \sim f \sim O(\epsilon^2)$, $v/Q \sim \epsilon$, $p_i \sim 1$, and $t \sim 1$. We therefore introduce order-one quantities $\bar{g} = g/\epsilon^2$, $\bar{f} = f/\epsilon^2$, $\bar{Q} = \epsilon Q/v$, in terms of which the leading-order stress-balance equations and the kinematic condition simplify to

$$-3R^2R' - 4\bar{g}R' + 4\bar{g}'R - 4\bar{f}R = -\frac{\sigma' R^2}{\bar{Q}}, \tag{5.8}$$

$$(p_i - 1)R^2 - 4\bar{g} = \frac{\sigma R}{\bar{Q}}, \tag{5.9}$$

$$R_t + zR' = \frac{2\bar{g}}{R} - \tfrac{1}{2}R. \tag{5.10}$$

The mass-source density $\bar{g}$ can be eliminated from equation (5.10) by using (5.9), which leads to the evolution equation

$$\frac{\partial R}{\partial t} + zR' + R = \tfrac{1}{2}\left(p_i R - \frac{\sigma}{\bar{Q}}\right), \tag{5.11}$$

for R. When σ is constant, this equation is equivalent on rescaling to the evolution equation in Hinch (1980). The tangential stress-balance equation (5.8) decouples from equation (5.11), and can be regarded as a relation for the Stokeslet density $\bar{f}$, if required, while equation (5.9) provides a relation for $\bar{g}$.

An equation for evolution of surfactant is obtained from (5.4) by estimating the velocity terms using (3.1) and (3.2) and the expansion of the integrals $I_{m,n}(\cdot)$. After incorporating the above scalings for f and g, we find

$$\frac{\partial \Gamma}{\partial t} + \frac{1}{R}\frac{\partial}{\partial z}(zR\Gamma) + \frac{\Gamma}{R}\left[\frac{2\bar{g}}{R} - \tfrac{1}{2}R - R'z\right] = 0. \tag{5.12}$$

The density $\bar{g}$ is eliminated from this last equation using the normal stress-balance equation (5.9), to give

$$\frac{\partial \Gamma}{\partial t} + z\frac{\partial \Gamma}{\partial z} + \frac{\Gamma}{2R}\left(p_i R - \frac{\sigma}{\bar{Q}}\right) = 0. \tag{5.13}$$

The pressure p_i is determined as follows. Differentiating the volume constraint (5.1) with respect to t, using equation (5.11) and the fact that $R(L(t), t) = 0$, together with the linear equation of state and the leading-order expression of conservation of surfactant (5.2), which is $v^2/\epsilon = \int_0^L \Gamma R \mathrm{d}z$, we obtain

$$p_i = 1 + \frac{3\epsilon^2}{2\bar{Q}v^3}\left(\int_0^{L(t)} R\mathrm{d}z - \frac{\beta v^2}{\epsilon}\right). \tag{5.14}$$

It follows directly from the two evolution equations for R and Γ, (5.11) and (5.13), that the leading-order expression for the total amount of surfactant is conserved.

The system of equations (5.11), (5.13) and (5.14) with the equation of state governs the time-dependent bubble shape and surfactant distribution away from the bubble endpoints, and is the main result of this section. The system is not closed, however, since the bubble half-length $L(t)$ which appears in (5.14) remains undetermined. It is found by a local analysis near the bubble endpoints, as shown in the next subsection.

5.2. *Endpoint expansions*

Evolution equations valid near the bubble endpoint $z = L(t)$ are derived by expanding the boundary conditions in powers of $L(t) - z$. The approach is to expand the integrals $I_{m,n}(\cdot)$ in a neighbourhood of the bubble endpoints, and the procedure we use here is similar to that employed by Tillett (1970). Details are given for $z \to L$; analogous expansions hold for $z \to -L$.

We assume the bubble has rounded ends, so that

$$R^2(z) = A_1(L - z) + A_2(L - z)^2 + \cdots \quad (A_1 \neq 0), \tag{5.15}$$

as $z \to L$. Substituting (5.15) into the time-dependent analogue of (3.4), in which $1 \mapsto L(t)$ in the limits of integration, Taylor expanding $\phi(\xi)$ about $\xi = L(t)$, and evaluating the resulting integrals, we find

$$\begin{aligned} I_{m,n}(z) \sim {} & \frac{-\phi(L)\delta^{m-n+1}}{m-n+1} + \frac{\phi'(L)\delta^{m-n+2}}{m-n+2} + O(\phi\delta^{m-n+3}) \\ & + \left[\phi(L)\delta^{m-n} + \frac{\epsilon^2 A_1 n\phi(L)\delta^{m-n-1}}{2(m-n-1)} + O(\phi\delta^{m-n+1}, \epsilon^2\phi\delta^{m-n})\right](L - z) \\ & + O[(L - z)^2] \end{aligned} \tag{5.16}$$

as $z \to L$, where it is understood that δ^p/p is replaced by $-\ln(1/\delta)$ in any term for which the exponent p of δ is zero.

The endpoint expansions (5.16) are substituted in equations (3.1)–(3.3) for the velocity components and equations (3.5)–(3.8) for the velocity gradient. Upon incorporating expansion (5.15) for the bubble shape, the kinematic condition takes the form

$$\dot{L} = L - 2f(L)\ln\delta + \frac{g(L)}{\delta} \tag{5.17}$$

at leading order $O((L - z)^{-1/2})$, where $f(L)$, $g(L)$ and δ are all time-dependent. At the next order in $L - z$, the kinematic condition (5.3) provides an equation for the evolution of A_1,

$$\dot{A}_1 = A_1\left\{-1 + \left(\tfrac{3}{2} - \frac{\epsilon^2 A_1}{2\delta}\right)\left(\frac{f(L)}{\delta} + \frac{g(L)}{2\delta^2}\right)\right\}. \tag{5.18}$$

The tangential and normal stress-balance equations, respectively, imply

$$\frac{6f(L)}{\delta} + \frac{3g(L)}{\delta^2} - \frac{\epsilon^2 A_1}{2\delta}\left(\frac{3f(L)}{\delta} + \frac{2g(L)}{\delta^2}\right) - 3 = -\frac{\nu}{Q}\sigma'(L), \tag{5.19}$$

$$p_i - \frac{6f(L)}{\delta} - \frac{2g(L)}{\delta^2} = \frac{4}{\epsilon^2 A_1}\frac{\nu}{Q}\sigma(L), \tag{5.20}$$

at leading order.

We suppose that the initial data for the unsteady evolution is a steady-state solution, as determined in § 3. This suggests the scalings $\sigma(L) \sim \epsilon$, $A_1 \sim 1$ and $\sigma'(L) \sim 1/\epsilon$, per equation (4.11). Control parameters are scaled according to the evolution equations that hold away from the bubble endpoints, as derived in § 5.1, so that $\nu/Q \sim \epsilon$ and $p_i \sim 1$. We envisage that the unsteady evolution is driven by a sudden increase of strain rate or decrease of ν/Q from its steady value of $O(1/\epsilon\ln(1/\epsilon))$ found in § 3, which causes a sudden decrease in p_i from $O(1/\epsilon^2\ln(1/\epsilon))$. We claim that these

scalings imply

$$\frac{f(L)}{\delta} \sim \frac{g(L)}{\delta^2} \sim 1. \tag{5.21}$$

To see this, suppose to the contrary that $f(L)/\delta \sim g(L)/\delta^2 \gg 1$. Then a non-trivial leading-order balance in equations (5.19) and (5.20) requires that $\epsilon^2 A_1/(2\delta) \sim 1$. A leading-order balance in equations (5.18)–(5.20) yields three distinct relations for the two quantities $f(L)/\delta$ and $g(L)/\delta^2$ which cannot be simultaneously satisfied. Similarly, if we suppose that $f(L)/\delta \sim g(L)/\delta^2 \ll 1$, then the resulting expression for p_i in equation (5.20) will be inconsistent with (5.14). Therefore, substituting the scaling (5.21) into (5.17) and recalling that $\delta \ll 1$, we find that the leading-order evolution equation for the bubble half-length is given by

$$\dot{L}(t) = L. \tag{5.22}$$

In physical terms, this states that the part of the surface in a neighbourhood of the bubble tips that is covered with diffusion-free surfactant is pulled along by the imposed flow, unperturbed, at speed $u_z = z$.

5.3. *Numerical solutions*

A closed system of slender-bubble evolution equations is given by (5.11), (5.13), (5.14) and (5.22), with the equation of state $\sigma = 1 - \beta\Gamma$. These are solved numerically, starting from a deformed steady state with $\beta = 0.5$ and $\epsilon = 0.0134$, which is the smallest value of ϵ for a steady surfactant-covered bubble, as determined from equation (3.38). The unsteady evolution is driven by a large far-field strain, with $\bar{Q} = 1$ and, from (3.36), $\nu = \epsilon^{2/3}$, which implies that the capillary number is $Q = \epsilon^{-1/3}$.

The result of the simulation is shown in figure 6, which shows the time-evolution of the upper-right-hand quadrant of a four-fold symmetric bubble. The initial slender-bubble shape is given by the leftmost curve in the figure, and we note that here the r-axis is in the scaled variable, so that when z and t are zero, R is unity. The evolving bubble surface is shown at subsequent times $t > 0$.

During the initial phase of deformation, surfactant is swept toward the bubble ends or poles, at which the bubble surface is stagnant, so that it is pulled along by the imposed flow, leading to a filamenting instability or tip-streaming. The filament tips move at the velocity of the imposed extensional flow, which is equal to the z-location of the tips. Figure 6(b) depicts the surfactant concentration $\Gamma(z)$ on the bubble surface at time $t = 3.5$. Note that over most of the main body of the bubble, the surfactant concentration is near zero, while on the filaments it is large. This is due to the outer straining field sweeping surfactant from the main body and onto the filaments and due to the relatively small surface area of the filaments, which combine to produce a high surfactant concentration there.

Figure 6 shows that the 'clean' main-bubble body eventually has a form that is reminiscent of the steady pointed shapes of Buckmaster (1972). Hinch (1980) has considered the evolution of a clean slender bubble in an axisymmetric straining flow, and found that there are 'shape preserving' solutions in the form of polynomials in z with time-dependent coefficients. One such polynomial solution is of the form of the steady (stable) Buckmaster bubble, but with time-dependent coefficients. In our scaling, this Hinch polynomial solution to equation (5.11) for a clean bubble with $\sigma = 1$ is

$$R(z, t) = A(t)(1 - z^2/L^2), \tag{5.23}$$

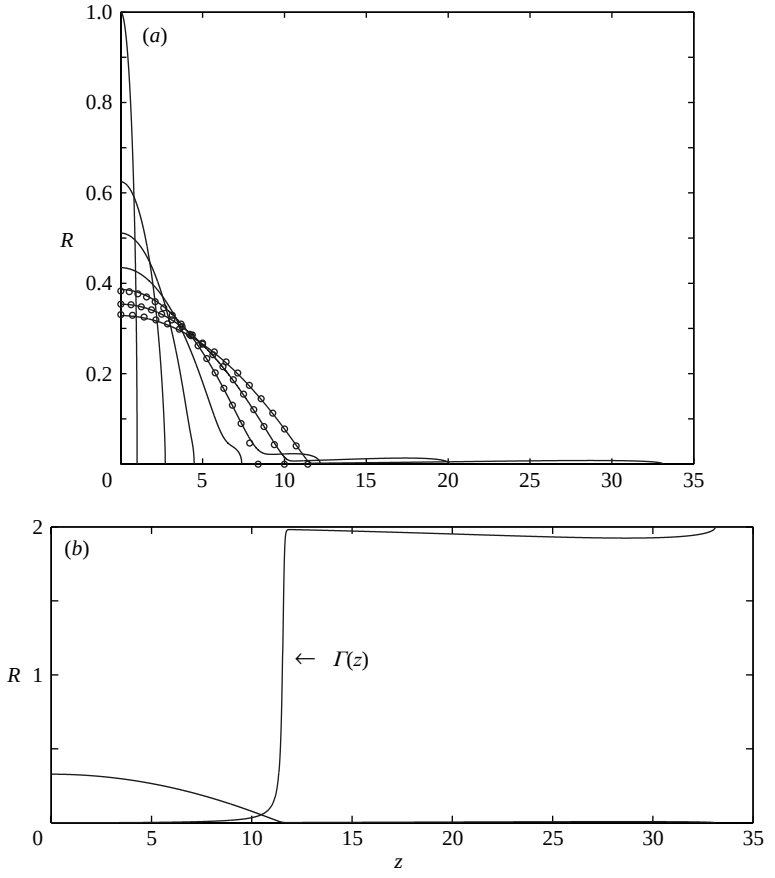

FIGURE 6. (*a*) Bubble shapes $R(z, t)$ for $t = 0.0, 1.0, 1.5, 2.0, 2.5, 3.0, 3.5$. Note the tip-streaming thread at the right-hand endpoint. ○, the clean-bubble solution given by (5.23) and (5.24), with $A(0)$ determined as described in the text. (*b*) Bubble shape $R(z, t)$ and surfactant concentration $\Gamma(z, t)$ at $t = 3.5$.

where A and L satisfy

$$A(t) = \frac{1}{4\bar{Q}} + \left(A(0) - \frac{1}{4\bar{Q}}\right) \exp\left(-\tfrac{1}{2}t\right), \quad L = \frac{5}{4}\frac{\nu^3}{\epsilon^2 A(t)^2}. \tag{5.24}$$

The relation for A follows from substituting equation (5.23) into (5.11), and that for L follows from consideration of volume conservation (5.1). Within the class of solutions investigated by Hinch (1980), (5.23) is of particular significance, since it approaches the steady solution of Buckmaster (1972) in the limit $t \to \infty$, and is stable to all perturbations of the form $c(t)z^m$ for even integers $m > 2$.

The circles in figure 6(*a*) represent the bubble profile given by (5.23) and (5.24) at three different times. The parameter $A(0)$ is determined by fitting (5.23) to the main-bubble body of the tip-streaming solution at time $t = 2.5$. The markers at subsequent times $t = 3.0,\ 3.5$ are then generated from (5.23) and (5.24), and show good agreement with the bubble profiles as found in the simulation with surfactant. This suggests that for $t \gtrsim 2.5$ the main body evolves essentially as though it were a clean bubble, and is approaching the steady stable Buckmaster profile.

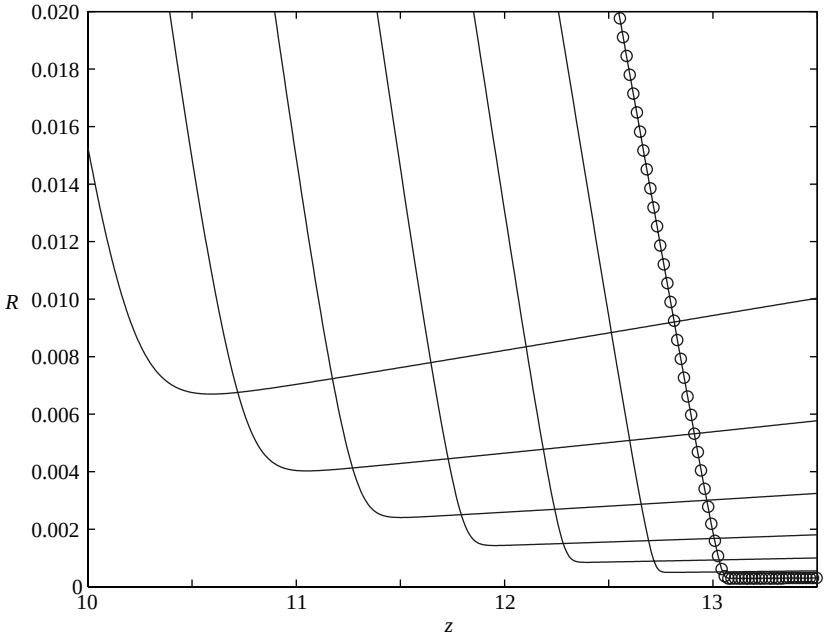

FIGURE 7. Evolution of the local minimum in R at the point where the main bubble joins the tip-streaming thread. The interface is shown at times $t = 3.0 - 4.2$ in increments of 0.2. ○, the numerical grid-points at the final time, indicating that the minimum is well-resolved.

Figure 7 shows a close-up of the interface shape near a local minimum that develops in R at some time $t > 0$. The interface tends to a double cone-shape, where the left-cone angle is found to approach that of the stable steady Buckmaster bubble, for which $\epsilon R' = -1/(40Q^3)$. The profiles are suggestive of an eventual pinch-off, with shallow cone angles that are consistent with the slenderness assumption. A more detailed study of possible pinch-off will appear in a future paper.

6. Conclusion

Slender-body theory has been used to study the steady-state deformation and time-dependent evolution of an axisymmetric bubble in zero-Reynolds-number extensional flow, when insoluble and surface-diffusion-free surfactant resides on the bubble surface. The presence of surfactant introduces a number of important differences compared to the theory for clean bubbles developed by, e.g. Taylor (1964), Buckmaster (1972, 1973), Acrivos & Lo (1978) and others. In the limit of zero surface diffusion, insoluble surfactant immobilizes the surface of a steady bubble. The resulting scalings for the Stokeslet and source terms, f and g, that determine the flow exterior to the bubble are more like those for flow around a solid object (Tillett 1970) than a clean bubble. At sufficiently large bubble deformation, the solution is distinguished by the development of a surfactant-free, or clean, central part accompanied by stagnant surfactant-caps at the ends, with different scalings for f and g on each region. A local analysis indicates that a bubble with surfactant is rounded at its endpoints, in contrast to the pointed ends of a clean bubble. An additional non-uniformity at the edge of the surfactant-cap, or stick–slip problem, is not resolved.

Perhaps the most important difference is that, in the absence of surfactant, steady slender-bubble solutions exist for arbitrarily large capillary number, whereas in the presence of surfactant, we find a critical capillary number above which steady solutions no longer exist. This follows from analytical expressions which describe steady solution branches for surfactant-covered (see equation (3.37)) and stagnant-cap bubbles (equation (3.70)). The value of the critical capillary number, as determined from our asymptotic theory, compares well with that determined by boundary-integral numerical simulations of the Stokes equations and with experiment.

Equations governing the time-evolution of a slender inviscid bubble with surfactant have also been derived. The equations are valid for large capillary number, satisfying the scaling $Q = G\mu a/\sigma_0 \sim \epsilon^{-1/3}$. The time-dependent equations are, to the best of our knowledge, the first to be derived for slender bubbles with rounded endpoints. Since the small-slope assumption underlying slender-body theory breaks down at the endpoints, a local analysis is required to close the system of governing equations. Numerical simulations of these slender evolving bubble equations show solutions that exhibit tip-streaming. The simulations indicate that surfactant is swept from the main body of the bubble and onto tip-streaming filaments that emerge from the bubble poles or endpoints. The main body of the bubble then evolves in a manner similar to the clean slender-bubble solutions of Hinch (1980).

Several physical effects have been neglected in the current analysis, including interior fluid viscosity, fluid inertia and surfactant solubility. Many of these effects can be incorporated into a slender-bubble analysis, as has been done by Acrivos & Lo (1978) for a clean bubble, and this will be the subject of future work. We expect that the solutions presented in this paper can play the role of a 'base state' from which additional physical effects can be investigated through a perturbative approach.

The authors gratefully acknowledge support from NSF grants DMS-0420590 and (M.S.) DMS-0104350.

Appendix

A.1. *Approximation of the integral* $I_{m,n}(\phi)$

An exact solution of the Stokes equations can be written in terms of an integral of a distribution of point forces or Stokeslets on the boundaries of the flow region, and outside a body that is slender, the role of the Stokeslet distribution on the boundary can be approximated by distributions of Stokeslets and point mass sources on the body centreline $r = 0$. This leads to representation of the dependent variables in terms of integrals of the form

$$I_{m,n}(\phi) = \int_a^b k_{mn}(\xi, r, z)\phi(\xi)\,\mathrm{d}\xi \quad \text{where} \quad k_{mn} = \frac{(z-\xi)^m}{(r^2+(z-\xi)^2)^{n/2}},$$

for integer $m = 0, 1, \cdots$ and $n = 1, 3, \cdots$, see, for example, Leal (1992). A general, systematic method for deriving an asymptotic expansion for integrals of this type near and on the body surface as $r \to 0$ for an arbitrary function $\phi(\xi)$ has been given by Handelsman & Keller (1967), and we outline it here.

When $r = 0$ and $m < n$, the kernel k_{mn} in the integral is singular such as $(z - \xi)^m/|z - \xi|^n$. This suggests that for small r, there is a dominant local contribution to the integral from a neighbourhood of $\xi = z$, which contains the first few terms in the Taylor expansion of $\phi(\xi)$ at z, provided $\phi(\xi)$ is smooth there, whereas away from $\xi = z$, the kernel is approximated by its binomial expansion for small r.

The approximation procedure is to add and subtract to k_{mn} the first term in its binomial expansion for small r, namely $(z-\xi)^m/|z-\xi|^n$. This one term approximates the kernel well, away from $\xi=z$, and generates the largest non-local approximation to $I_{m,n}(\phi)$. However, for $m<n$, its singular behaviour at $\xi=z$ gives an integral that diverges unless a sufficient number of terms in the Taylor expansion of $\phi(\xi)$ about $\xi=z$ are subtracted from $\phi(\xi)$ to make the difference tend to zero as $(z-\xi)^{n-m}$. This requires that we add and subtract $p=n-m$ terms of its Taylor expansion to $\phi(\xi)$.

The exact expression that results is given by

$$\begin{aligned} I_{m,n}(\phi) &= \int_a^b \left(\sum_{j=0}^{p-1} \phi^{(j)}(z) \frac{(\xi-z)^j}{j!} + \left[\phi(\xi) - \sum_{j=0}^{p-1} \phi^{(j)}(z) \frac{(\xi-z)^j}{j!} \right] \right) \\ &\quad \times \left(\frac{(z-\xi)^m}{(r^2+(z-\xi)^2)^{n/2}} - \frac{(z-\xi)^m}{|z-\xi|^n} + \frac{(z-\xi)^m}{|z-\xi|^n} \right) \mathrm{d}\xi \qquad \text{(A 1)} \\ &= \sum_{j=0}^{p-1} \frac{(-1)^j \phi^{(j)}(z)}{j!} w_{m+j,n}(r,z) + \int_a^b \left[\phi(\xi) - \sum_{j=0}^{p-1} \phi^{(j)}(z) \frac{(\xi-z)^j}{j!} \right] \\ &\quad \times \frac{(z-\xi)^m}{|z-\xi|^n} \, \mathrm{d}\xi + \mathscr{R}. \end{aligned}$$

Here, the integrals

$$w_{l,n}(r,z) = \int_a^b \frac{(z-\xi)^l}{(r^2+(z-\xi)^2)^{n/2}} \, \mathrm{d}\xi$$

that appear in the local contributions to the expansion are known in terms of elementary functions of r, z, a and b. For example, the integrals $I_{0,1}(f)$ and $I_{2,3}(f)$ that appear in the no-slip boundary condition $u_z=0$ and equation (3.10) require $w_{0,1}$ and $w_{2,3}$, which are given by

$$\begin{aligned} w_{0,1} &= -2\ln r + \ln(b-z+((b-z)^2+r^2)^{1/2}) + \ln(z-a+((z-a)^2+r^2)^{1/2}), \\ w_{2,3} &= w_{0,1} - \frac{b-z}{((b-z)^2+r^2)^{1/2}} - \frac{z-a}{((z-a)^2+r^2)^{1/2}}. \end{aligned}$$

The remainder is given by

$$\mathscr{R} = \int_a^b \left(\frac{(z-\xi)^m}{(r^2+(z-\xi)^2)^{n/2}} - \frac{(z-\xi)^m}{|z-\xi|^n} \right) \left[\phi(\xi) - \sum_{j=0}^{p-1} \phi^{(j)}(z) \frac{(\xi-z)^j}{j!} \right] d\xi \qquad \text{(A 2)}$$

and is of order $O(r)$ times the order of ϕ as $r \to 0$. The approximation scheme can be pursued to higher order, by introducing the next term in the binomial expansion of $k_{m,n}$, either at the beginning of (A 1) or in the remainder (A 2).

A.2. *The singular behaviour of $f^+(z)$ as $z \to a^+$.*

Although we do not address the solution of the 'stick–slip' problem that occurs in a neighbourhood of the surfactant-cap boundaries at $z=\pm a$, its solution would require asymptotic matching with the solution constructed here. To this end, we present the most singular part of the Stokeslet distribution f^+ on the right-hand surfactant-cap as $z \to a^+$.

Let the leading-order singular part of f_j^+, which was defined at (3.41), be denoted by $\check{f}_j^+$. We show by induction that

$$\check{f}_j^+ = \mu_j z \ln^j(z-a) \quad (j=0,1,2,\ldots), \tag{A 3}$$

where μ_j satisfy the recusion relation

$$\mu_j = -\mu_{j-1}\left(1-\frac{1}{2j}\right) \quad (j=1,2,\ldots), \quad \text{with} \quad \mu_0 = -\frac{1}{4}. \tag{A 4}$$

The calculation of § 3.2 at equations (3.57) and (3.60) has shown that $\mu_0 = -1/4$ and $\mu_1 = 1/8$. Assume that (A 3) and (A 4) hold for $1 \leqslant j \leqslant n$. Successive iterates of $\check{f}^+$ are constructed from equation (3.52), and in particular the equation for $\check{f}_{n+1}^+$ is

$$2\check{f}_{n+1}^+ + \mu_n z \ln^{n+1}(z-a) + \mu_n \int_a^1 \frac{\xi \ln^n(\xi-a) - z\ln^n(z-a)}{|z-\xi|}\,\mathrm{d}\xi = 0, \tag{A 5}$$

for $z \in (a,1)$. In deriving (A 5) from (3.52) we have used the fact that R_j, for $j=1,\ldots,n$, is less singular than $\check{f}_n^+$. This follows from equation (3.56), or on recognizing that each R_j is bounded and continuous at $z=a$. Also, we note that the last integral in (3.52) over the left-hand surfactant-cap is not singular as $z \to a^+$.

After writing $\xi = z + \xi - z$ for the first occurrence of ξ in the integral in (A 5), the most singular part of the integral is seen to be given by

$$\begin{aligned} s(z) &= z\int_a^1 \frac{\ln^n(\xi-a) - \ln^n(z-a)}{|z-\xi|}\,\mathrm{d}\xi \\ &= z\left(\int_a^z \frac{\ln^n(\xi-a)-\ln^n(z-a)}{z-\xi}\,\mathrm{d}\xi + \int_z^1 \frac{\ln^n(\xi-a)-\ln^n(z-a)}{\xi-z}\,\mathrm{d}\xi\right) \\ &\equiv s_1(z) + s_2(z). \end{aligned}$$

The most singular part of $s_1(z)$ is of order $O(\ln^{n-1}(z-a))$, and the most singular part of $s_2(z)$ is identical to that of the integral

$$\int_z^1 \frac{\ln^n(\xi-a)-\ln^n(z-a)}{\xi-a}\,\mathrm{d}\xi,$$

which is readily found. The most singular part of $s(z)$ is therefore found to satisfy

$$s(z) \sim s_2(z) \sim \left(1-\frac{1}{n+1}\right) z\ln^{n+1}(z-a),$$

which, substituted into (A 5), shows the validity of (A 3) and (A 4) for $j=n+1$.

The recursion relation (A 4) implies that

$$\mu_j = (-1)^{j+1}\frac{1}{4}\left(\frac{1}{2}\frac{3}{4}\frac{5}{6}\cdots\frac{2j-1}{2j}\right) = (-1)^{j+1}\frac{(2j-1)!}{2^{2j+1}j!(j-1)!} \quad \text{for } j=1,2,\ldots, \tag{A 6}$$

with $\mu_0 = -1/4$, and (A 3) shows that the most singular part of f^+, to all integer powers of $\ln(1/\epsilon)$, is given by

$$f^+ \sim \sum_{j=0}^{N} \mu_j \frac{z\ln^j(z-a)}{\ln^{j+1}(1/\epsilon)}. \tag{A 7}$$

The most singular part of g^-, f^- and g^+ then follows from the relations (3.50), (3.51) and (3.54), respectively.

REFERENCES

Acrivos, A. & Lo, T. S. 1978 Deformation and breakup of a single slender drop in an extensional flow. *J. Fluid Mech.* **86**, 641–672.

Acrivos, A. 1983 The breakup of small drops and bubbles in shear flows. *Ann. NY Acad. Sci.* **404**, 1–11.

Barthes-Biesel, D. & Acrivos, A. 1973 Deformation and burst of a liquid droplet freely suspended in a linear shear field. *J. Fluid Mech.* **61**, 1–21.

Bentley, B. J. & Leal, L. G. 1986 A computer-controlled four-roll mill for investigations of particle and drop dynamics in two-dimensional linear shear flows. *J. Fluid Mech.* **167**, 219–240.

Buckmaster, J. D. 1972 Pointed bubbles in slow viscous flow. *J. Fluid Mech.* **55**, 385–400.

Buckmaster, J. D. 1973 The bursting of pointed drops in slow viscous flow. *Trans. ASME E:J. Appl. Mech.* **40**, 18–24.

De Bruijn, R. A. 1993 Tipstreaming of drops in simple shear flows. *Chem. Engng Sci.* **48**, 277–284.

Eggers, J. 1997 Nonlinear dynamics and breakup of free-surface flows. *Rev. Mod. Phys.* **69**, 865–929.

Eggleton, C. D., Pawar, Y. P., & Stebe, K. J. 1999 Insoluble surfactants on a drop in an extensional flow: a generalization of the stagnated surface limit to deforming interfaces. *J. Fluid Mech.* **385**, 79–99.

Eggleton, C. D., Tsai, T. M. & Stebe, K. J. 2001 Tip streaming from a drop in the presence of surfactant. *Phys. Rev. Lett.* 87(4), 048302.

Grace, H. P. 1982 Dispersion phenomena in high viscosity immiscible fluid systems and application of static mixers as dispersion devices in such systems. *Chem. Engng. Commun.* **14**, 225–277.

Handelsman, R. A. & Keller, J. B. 1967 Axially symmetric potential flow around a slender body. *J. Fluid Mech.* **28**, 131–147.

Hinch, E. J. 1980 The evolution of slender inviscid drops in an axisymmetric straining flow. *J. Fluid Mech.* **101**, 545–553.

Howison, S. D., Morgan, J. D. & Ockendon, J. R. 1997 A class of codimension-two free boundary problems. *SIAM Rev.* **39**, 221–253.

Hu, Y. T., Pine, D. J. & Leal, L. G. 2000 Drop deformation, breakup, and coalescence with compatibilizer. *Phys. Fluids* **12**, 484–489.

Janssen, J. J. M., Boon, A. & Agterof, W. G. M. 1994 Influence of dynamic interfacial properties on droplet breakup in plane hyperbolic flow. *AIChE. J.* **40**, 1929.

Janssen, J. J. M., Boon, A. & Agterof, W. G. M. 1997 Influence of dynamic interfacial properties on droplet breakup in simple shear flow. *AIChE. J.* **43**, 1436–1447.

Jeffery, G. B. 1922 The motion of ellipsoidal particles immersed in a viscous fluid. *Proc. R. Soc. Lond.* A **102**, 161–179.

Leal, L. G. 1992 *Laminar Flow and Convective Transport Processes: Scaling Principles and Asymptotic Analysis.* Butterworth–Heinemann.

Milliken, W. J., Stone, H. A. & Leal, L. G. 1993 The effect of surfactant on transient motion of Newtonian drops. *Phys. Fluids* A **5**, 69–79.

Rallison, J. M. 1984 The deformation of small viscous drops and bubbles in shear flows. *Annu. Rev. Fluid Mech.* **16**, 45–66.

Rumscheidt, F. D. & Mason, S. G. 1961 Particle motions in sheared suspensions XII. Deformation and burst of liquid drops in shear and hyperbolic flow. *J. Colloid. Interface. Sci.* **16**, 238–261.

Sadhal, S. S. & Johnson, R. E. 1983 Stokes flow past bubbles and drops partially coated with thin films. Part 1. Stagnant cap of surfactant film – exact solution. *J. Fluid Mech.* **126**, 237–250.

Sherwood, J. D. 1984 Tip streaming from slender drops in a nonlinear extensional flow. *J. Fluid Mech.* **144**, 281–295.

Siegel, M. 1999 Influence of surfactant on rounded and pointed bubbles in two dimensional Stokes flow. *SIAM J. Appl. Maths.* **59**, 1998–2027.

Stone, H. A. 1994 Dynamics of drop deformation and breakup in viscous fluids. *Annu. Rev. Fluid Mech.* **26**, 65–102.

Stone, H. A. & Leal, L. G. 1990 The effects of surfactants on drop deformation and breakup. *J. Fluid Mech.* **222**, 161–186.

Taylor, G. I. 1934 The formation of emulsions in definable fields of flow. *Proc. R. Soc. Lond.* A **146**, 501–523.

Taylor, G. I. 1964 Conical free surfaces and fluid interfaces. *Proc. 11th Intl Cong. of Appl. Mech. Munich*, pp. 790–796.

Tillet, J. P. J. 1970 Axial and transverse Stokes flow past slender axisymmetric bodies. *J. Fluid Mech.* **44**, 401–417.

Torza, S., Cox, R. G. & Mason, S. G. 1972 Particle motions in sheared suspensions XXVII. Transient and steady deformation and burst of liquid drops. *J. Colloid. Interface. Sci.* **38**, 395–411.

Wong, H., Rumschitzki, D. & Maldarelli, C. 1996 On the surfactant mass balance at a deforming fluid interface. *Phys. Fluids* A **8**, 3203–3204.

Youngren, G. K. & Acrivos, A. 1976 On the shape of a gas bubble in a viscous extensional flow. *J. Fluid Mech.* **76**, 433–442.